



## Fascin regulates protrusions and delamination to mediate invasive, collective cell migration *in vivo*

Maureen C. Lamb, Kelsey K. Anliker, and Tina L. Tootle\*

Anatomy and Cell Biology, University of Iowa Carver College of Medicine, Iowa City, IA,  
52242

\*Corresponding author: [tina-tootle@uiowa.edu](mailto:tina-tootle@uiowa.edu)

Running title: Fascin regulates border cell migration

Keywords: Drosophila, Fascin, border cell, Enabled, E-Cadherin, migration

This project is supported by National Institutes of Health R01GM116885

Accepted Articles are accepted, unedited articles for future issues, temporarily published online in advance of the final edited version.

## Abstract

### Background

The actin bundling protein Fascin is essential for developmental cell migrations and promotes cancer metastasis. In addition to bundling actin, Fascin has several actin-independent roles; how these other functions contribute to cell migration remains unclear. Border cell migration during *Drosophila* oogenesis provides an excellent model to study Fascin's various roles during invasive, collective cell migration.

### Results

On-time border cell migration during Stage 9 requires Fascin (*Drosophila* Singed). Fascin functions not only within the migrating border cells, but also within the nurse cells, the substrate for this migration. Fascin genetically interacts with the actin elongation factor Enabled to promote on-time Stage 9 migration and overexpression of Enabled suppresses the defects seen with loss of Fascin. Loss of Fascin results in increased, shorter and mislocalized protrusions during migration. Additionally, loss of Fascin inhibits border cell delamination and increases E-Cadherin (*Drosophila* Shotgun) adhesions on both the border cell clusters and nurse cells.

### Conclusions

Overall, Fascin promotes on-time border cell migration during Stage 9 and contributes to multiple aspects of this invasive, collective cell migration, including both protrusion dynamics and delamination. These findings have implications beyond *Drosophila*, as border cell migration has emerged as a model to study mechanisms mediating cancer metastasis.

## Introduction

Fascin is an actin-binding protein that bundles or cross-links actin filaments<sup>1,2</sup> to promote cell motility and invasion through the formation of filopodia and invadopodia.<sup>3-5</sup> While Fascin does promote cell migration in this actin-dependent manner, novel actin-independent roles of Fascin have been discovered.<sup>6-8</sup> Fascin directly binds the Linker of the Nucleoskeleton and Cytoskeleton (LINC) complex, which mediates mechanotransduction. Perturbing this interaction impairs nuclear shape deformations essential for single-cell invasive migration.<sup>7</sup> Fascin also binds to microtubules and loss of this interaction increases the stability of cellular adhesions, causing slower migration.<sup>6</sup> Additionally, Fascin interacts with Protein Kinase C (PKC), LIM kinases (LIMKs), and, notably, Enabled (Ena).<sup>8-11</sup> Ena is an actin elongation factor, and *in vitro* Ena processivity is increased on Fascin-bundled actin.<sup>9,12</sup> These studies illustrate Fascin has multiple functions within the cell that regulate cell migration.

Fascin is important for both developmental cell migrations and cancer metastasis.<sup>2,13,14</sup> Fascin controls cell migration during development including growth cone extension, dendrite formation, and in embryonic fibroblasts.<sup>15,16</sup> Fascin is also highly upregulated in certain types of cancer, and elevated expression is associated with increased invasiveness, aggressiveness and mortality.<sup>2,10,17</sup> While Fascin has been studied in the contexts of 2D migration and single cell 3D migration, the roles of Fascin in invasive, collective cell migration have yet to be investigated.<sup>5,7</sup>

*Drosophila* oogenesis – specifically border cell migration – is an ideal model to study invasive, collective cell migration. *Drosophila* oogenesis has 14 developmental stages of egg chambers or follicles.<sup>18</sup> Each follicle is composed of a single oocyte, 15 germline-derived nurse cells, and a layer of somatic epithelial cells, or follicle cells, surrounding the outside. During Stage 9 (S9) of follicle development, a group of follicle cells at the anterior end are specified to become border cells. This group of 8-10 border cells delaminates from the epithelium and migrates between the nurse cells to reach the nurse cell-oocyte boundary.<sup>19,20</sup> Delamination is a highly regulated process in which the border cells must maintain cellular adhesions, such as E-Cadherin (*Drosophila* Shotgun), amongst themselves, but sever adhesions with their neighboring

follicle cells and nurse cells.<sup>21</sup> Additionally, border cell migration is very dynamic with protrusions extending and retracting to move the cluster.<sup>22,23</sup> Upon completing its migration, the border cells contribute to the formation of the micropyle, the structure through which sperm fertilize the egg.<sup>18,24</sup> Importantly, the migrating border cells highly express Fascin.<sup>25</sup> Therefore, we can study the role of Fascin (*Drosophila* Singed) in invasive, collective cell migration *in vivo* using the simple and genetically tractable model of border cell migration.

Here we find that Fascin plays a critical role in regulating border cell migration. Using a new quantification method to assess border cell migration during S9, we find loss of Fascin results in significant delays in migration. Surprisingly, Fascin is required in both the border cells and germline cells to mediate on-time border cell migration during S9. Dominant genetic interactions reveal Fascin and Ena work together to regulate border cell migration, and somatic overexpression of Ena suppresses migration defects in *fascin* mutants. Live imaging reveals that loss of Fascin results in border cell clusters with more protrusions, emerging from all sides, that are shorter in length and duration. These alterations culminate in the border cell clusters of *fascin*-null follicles migrating slower than controls. We hypothesize these defects are due, in part, to Fascin's role in regulating Ena. Fascin also regulates border cell delamination. In *fascin*-null mutants, the clusters take longer to delaminate, and display increased membrane localization of E-Cadherin. Overall, our data reveal that Fascin regulates multiple aspects of border cell migration, including both protrusion dynamics and delamination. These findings lead to the model that Fascin regulates invasive, collective cell migration through modulating cellular protrusions by bundling actin and regulating both cellular protrusions and adhesions to control the initiation of migration.

## Results

### On-time border cell migration during Stage 9 requires Fascin

Previously, it was reported that loss of Fascin (*Drosophila* Singed) does not affect border cell migration.<sup>25</sup> This analysis showed that border cells of *fascin*-null mutants completed their

migration between the nurse cells and reached the nurse cell-oocyte boundary by Stage 10A (S10A)<sup>25</sup>; we have reproduced these findings (data not shown). These findings are surprising as Fascin is highly expressed in the border cells<sup>25</sup> and regulates many types of cell migration.<sup>1,2</sup> Thus, we hypothesized that while border cells reach the nurse cell-oocyte boundary by S10A, border cell migration may be altered during S9 in *fascin* mutants.

During S9, the follicle undergoes dramatic morphological changes and increases in size (Figure 1A). At the beginning of S9, the entire follicle is surrounded by a uniform layer of follicle cells. As the follicle grows in size, ~50 anterior follicle cells become squamous, stretch follicle cells, while the remaining outer follicle cells become progressively localized to the posterior. By the end of S9, these outer follicle cells only cover the oocyte (Figure 1A). These follicle cell changes are coordinated with border cell migration. At any point during S9, the distance the border cells have migrated is approximately equal to the distance the outer follicle cells are from the anterior of the follicle (Figure 1A). Thus, delayed or accelerated migration of the border cells during S9 can be quantitatively assessed by comparing their location relative to that of the outer follicle cells.

To quantify border cell migration during S9, we measure the distance the border cells have migrated in microns (termed border cell distance) and the distance of the outer follicles from the anterior end in microns (termed outer follicle cell distance). We divide the border cell distance by the outer follicle cell distance to calculate what we term the migration index (Figure 1A). For the purposes of this paper, when we refer to on-time or delayed migration we are specifically referencing the state of border cell migration during S9. A migration index of ~1 indicates on-time migration, while a value less than 1 indicates delayed migration and a value greater than 1 indicates accelerated migration (Figure 1A). To assess border cell migration, we performed immunofluorescent staining for Hts and FasIII; this stain will be referred to throughout the paper as the border cell migration stain. This stain labels both border cells and outer follicle cells and enables us to quantify the migration index (Figure 1B-C). In the example quantification shown in Figure 1B the wild-type follicle has a border cell distance of 92.56μm

and an outer follicle cell distance of 94.64 $\mu$ m, leading to a migration index of 0.97 (0.97=92.56 $\mu$ m /94.64 $\mu$ m), indicating on-time migration. Conversely, the *fascin*-null follicle has a border cell distance of 36.93 $\mu$ m and an outer follicle cell distance of 102.02 $\mu$ m, leading to migration index of 0.36 (0.36=36.93 $\mu$ m /102.02 $\mu$ m), indicating delayed migration (Figure 1C). This quantification method allows for the identification of defects in migration during S9 that may not be apparent at S10. Specifically, it allows the identification and analysis of border cell migration regulators that contribute to the migration but have more subtle effects, such as S9 defects, than a failure to complete migration by S10. Lack of a S10 phenotype may arise due to compensation by related proteins or activities during only particular periods of migration. However, such factors still contribute to migration and may have physiological effects.

We quantified the migration index in wild-type and *fascin* mutant follicles, in a genotypically blinded manner (Figure 2). Two different null alleles of *fascin* were used, *fascin*<sup>sn28</sup> and *fascin*<sup>snX2</sup>.<sup>25,26</sup> Wild-type S9 follicles display on-time border cell migration with an average migration index of 1.03 and normal distribution between 0.30 and 1.69 (Figure 2A, D). Partial loss of Fascin also results in on-time border cell migration with average migration indices of 1.00 for *fascin*<sup>sn28/+</sup> and 0.97 for *fascin*<sup>snX2/+</sup> (Figure 2B, D and data not shown). Loss of Fascin by both homozygous (*fascin*<sup>sn28/sn28</sup> and *fascin*<sup>snX2/snX2</sup>) and transheterozygous *fascin* mutations (*fascin*<sup>sn28/snX2</sup> and *fascin*<sup>snX2/sn28</sup>; maternal allele is listed first) results in border cell clusters that are significantly delayed with average migration indices of 0.76 (p<0.0001), 0.82 (p=0.0002), 0.71 (p<0.0001), and 0.83 (p=0.0468), respectively (Figure 2C-D and data not shown).

Changes in the migration index could be due to defects in border cell migration or outer follicle cell morphogenesis. In regards to outer follicle cell morphogenesis, if the outer follicle cells are prematurely ahead of where they should be, it would result in a migration index of <1. To assess outer follicle cell morphogenesis, we analyzed the distance the outer follicle cells traveled versus overall follicle length, in wild-type and *fascin*-null follicles. In wild-type follicles, as the S9 follicles increase in length (which occurs throughout S9) there is a corresponding increase in outer follicle cell distance, meaning there is a positive relationship

between outer follicle cell distance and follicle length (Figure 2E, black open circles). If increased outer follicle cell distance was occurring in *fascin*-mutant follicles, we would expect a steeper slope in the relationship between outer follicle cell distance and follicle length. However, a very similar trend is observed in *fascin*-mutants compared to wild-type follicles (Figure 2E, blue circles). This finding indicates the outer follicle cells of the *fascin*-mutant follicle progress at the same rate as wild-type and the reduced migration index values (Figure 2D) are due to aberrant border cell migration during S9.

To further characterize the delayed migration due to loss of Fascin, we used our migration index measurements to assess border cell migration at different points during S9. As overall follicle length increases throughout S9, it is an indicator of what point during S9 a follicle is in. We measured the follicle length in the wild-type and *fascin*-null follicles, binned them into four groups (from early to late S9) and compared the average migration indicies (Figure 2F). The *fascin*-null follicles (all allelic combinations were combined) display significant delays in their migration index throughout the entirety of S9. These data indicate Fascin is required throughout the whole process of border cell migration.

### **Fascin is necessary in both the border cells and germline cells for on-time border cell migration**

We next sought to identify where Fascin is needed for border cell migration. During early oogenesis, Fascin is weakly expressed in the nurse cells, and is absent or extremely low in the follicle cells. During S9, this pattern remains, with the exception that Fascin is highly upregulated in the border cell cluster and a few posterior follicle cells (see Figure 4A).<sup>25</sup> Based on this expression pattern, Fascin could act in the border cells, the nurse cells, or both to regulate on-time border cell migration. Indeed, the nurse cells are the substrate upon which the border cells migrate and changes in nurse cell structure or stiffness perturb border cell migration.<sup>27,28</sup>

The UAS/GAL4 system<sup>29</sup> was used to express Fascin RNAi constructs to knockdown Fascin in specific cell types and determine the effects on border cell migration. Two different

Fascin RNAi lines were used (second chromosome: TRiP.HMJ21813 and third chromosome: TRiP.HMS02450) and yielded similar results; data presented uses the third chromosome line. We knocked down Fascin using *mat $\alpha$*  GAL4 (germline cell specific), *c355* GAL4 (somatic cell specific) or *c306* GAL4. *c306* GAL4 is largely expressed in the border cells during oogenesis but is also expressed in other cells, such as the stalk cells, posterior and anterior follicle cells, and follicle stem cells.<sup>30,31</sup> Since Fascin is expressed at very low levels in these cells compared to the border cells, we use the *c306* GAL4 as a border cell specific driver for Fascin. For all the GAL4 drivers, knockdown of Fascin was confirmed by immunostaining for Fascin (Figure 4A-C' and data not shown). Knockdown of Fascin in the germline cells causes significant border cell migration delays compared to the GAL4 driver only and RNAi only controls (Figure 3A-B, E; migration indices of 0.67 compared to 0.92 and 0.89, p<0.0001). Knockdown of Fascin in all somatic cells also causes significant border cell migration delays (Figure 3A, C, E; migration indices of 0.73 compared to 0.98 and 0.89, p<0.0001). Similarly, knockdown of Fascin in only the border cells causes delayed migration and the migration index is trending towards significantly different with a p-value of 0.051 (Figure 3A, D, E; migration indices of 0.82 compared to 0.94 and 0.89). This mild phenotype is likely due to insufficient knockdown of Fascin during migration, as Fascin is massively upregulated during border cell specification. Indeed, in the border cell knockdown high levels of Fascin are observed in the border cells at early stages of migration (Figure 4B-B') and diminishing levels at the later stages (Figure 4C-C'). Since the knockdown of Fascin in the border cells was variable, we repeated the border cell knockdown experiments by staining for Fascin and only quantifying S9 follicles that displayed sufficient knockdown in the border cells (Figure 4D-E). From these experiments, knockdown of Fascin in the border cells causes significant delays in border cell migration compared to controls (Figure 4F; migration indices of 0.68 compared to 0.97 and 0.93, p<0.0001). Together these findings indicate Fascin is necessary in both the border cells and germline for on-time border cell migration.

Since the border cells aid in forming the egg's micropyle, their migration is critical for female fertility.<sup>24</sup> Additionally, *fascin* mutant flies are female sterile.<sup>32</sup> We wanted to determine if knockdown of Fascin and delays in border cell migration also lead to defects in fertility. Knockdown of Fascin in the germline causes severe fertility defects with an average progeny per female of 5.14 compared to 26.9 and 39.3 for the GAL4 driver only and RNAi only controls (Figure 4G, p<0.0001). This finding was expected as Fascin is known to play an essential role in the germline during S10B of oogenesis.<sup>25</sup> Knockdown of Fascin in the somatic cells causes a significant reduction in female fertility with an average progeny per female of 20.0 compared to 30.0 and 29.3 for the GAL4 driver only and RNAi only controls, respectively (Figure 4G, p<0.05). Additionally, knockdown of Fascin using *c306* GAL4 causes a significant reduction in female fertility with an average progeny per female of 18.7 (Figure 4G, p<0.05). Given the expression patterns of Fascin and *c306* GAL4, in addition to the similar fertility defects when Fascin is knocked down in all somatic cells versus with *c306* GAL4, these results are consistent with the idea that delayed border cell migration during S9 leads to defects in follicle development and female fertility. However, we cannot exclude the possibility that reduction of Fascin in other cell types is contributing to the reduced fertility.

To further define the cell-specific roles of Fascin in border cell migration, the UAS/GAL4 system was used to express GFP-Fascin in specific cell types of *fascin* mutant follicles to determine where restoring expression rescues border cell migration. We expressed GFP-Fascin in the somatic cells (*c355* GAL4), the border cells (*c306* GAL4), the germline cells (*oskar* GAL4), or in both the germline and somatic cells ("Global GAL4", *actin5C* GAL4). Expression of GFP-Fascin in the somatic cells or the border cells of *fascin* mutant follicles restores border cell migration (Figure 5A-D, I; migration indices 0.97 compared to 0.70 [p=0.0036] and 0.90 compared to 0.60 [p<0.0001]). Conversely, expression of GFP-Fascin in the germline cells of *fascin* mutant follicles fails to rescue border cell migration (Figure 5E-F, I; migration indices of 0.75 compared to 0.70, p=0.63). This result was surprising given that RNAi knockdown of Fascin in the germline causes delayed migration (Figure 3A-B, E). We

hypothesized that these conflicting results may be due to the expression level induced by the germline GAL4, as Fascin is weakly expressed in the nurse cells during S9 (see Figure 4A).<sup>25</sup> Indeed, we find the germline GAL4 expresses GFP-Fascin in the germline at a much higher level than endogenous Fascin (data not shown). This high level of germline GFP-Fascin expression causes changes in border cell cluster morphology. The border cell cluster area increases significantly when GFP-Fascin is expressed in the germline of either wild-type or *fascin* mutant backgrounds compared to controls (Figure 6A-E). This finding suggests that the high expression level of Fascin in the germline affects the border cell cluster and may impair the rescue of border cell migration; it also suggests that Fascin levels in the germline must be tightly regulated to mediate on-time border cell migration. In attempt to recapitulate the endogenous expression levels of Fascin, we used a GAL4 driver that expresses weakly in the germline and strongly in the somatic cells (“Global GAL4”). Expression of Fascin using this GAL4 driver in *fascin* mutant follicles restores on-time border cell migration (Figure 5G-I; migration indices of 1.14 compared to 0.63; p<0.0001). Together these data support the model that Fascin acts both within the border cells and the nurse cells to regulate on-time border cell migration.

### Fascin genetically interacts with Ena to promote border cell migration

We next wanted to determine how Fascin regulates border cell migration. Recent findings demonstrate that Fascin cooperates with the actin elongation factor Ena to promote actin polymerization and filament formation *in vitro* by enhancing Ena processivity.<sup>9,12</sup> Additionally, loss of Ena causes border cell migration defects.<sup>33</sup> Based on these data, we tested the role of Ena downstream of Fascin in mediating border cell migration.

Dominant genetic interaction studies were used assess if Fascin and Ena interact during border cell migration. Reduced levels of Fascin (*fascin*-/+ or Ena (*ena*-/+) alone should be sufficient to maintain normal border cell migration. If Fascin and Ena function together to mediate border cell migration, then reduced levels of both (*fascin*-/+; *ena*-/+) will exhibit delayed border cell migration during S9. Partial loss of Fascin (Figure 2B, D and data not shown)

or two different *ena* alleles *ena*<sup>210/+</sup> (Figure 7A) and *ena*<sup>23/+</sup> (data not shown) exhibit on-time border cell migration (Figure 7C; migration indices of 1.00, 0.96, and 0.95, respectively). However, double heterozygotes of *fascin* with either *ena* allele (*fascin*-/+; *ena*-/+) cause significant border cell migration delays (Figure 7B-C; migration indices of 0.78 [p=0.045] and 0.68 [p=0.0015]). These dominant genetic interaction results indicate Fascin and Ena act together to promote border cell migration. We next wanted to address whether Ena acts upstream or downstream of Fascin. If Ena acts downstream of Fascin, then overexpression of Ena is predicted to suppress the border cell migration delay observed in *fascin*-null follicles. Indeed, expression of RFP-tagged Ena in the somatic cells (*c355 GAL4*) of *fascin* mutant follicles leads to on-time migration (Figure 7D-F; migration indices of 0.87 compared to 0.49; p<0.0001). These findings reveal that overexpression of Ena in the somatic cells, likely within the border cells, can compensate for the loss of Fascin. Together these data lead us to speculate that Fascin promotes Ena activity within the border cells to mediate migration, similar to how Fascin acts *in vitro*.<sup>9,12</sup>

### Fascin regulates protrusion dynamics of the migrating border cell cluster

Since Fascin and Ena genetically interact during border cell migration and this interaction is known to promote the formation of cellular protrusions in other systems<sup>9,12</sup>, we next investigated whether loss of Fascin affects border cell cluster protrusions using live imaging. We visualized border cell migration with membrane localized GFP expressed under the control of the *slbo* promoter (*slbo>mCD8-GFP*), which specifically labels the border cells and allows us to analyze cluster protrusions.

During migration, the border cell cluster typically forms one or two large protrusions that extend and retract from the leading edge of the cluster as it migrates.<sup>22,34</sup> In agreement with this, control follicles (*fascin*<sup>sn28/+</sup>) typically have one or two main protrusions extending and retracting from the front of the cluster (Figure 8A-A'', red arrowheads and Movie 1). Conversely, in *fascin*-null mutants (*fascin*<sup>sn28/sn28</sup>) the clusters extend many protrusions from their front, sides, and back (Figure 8B-B'', red arrowheads and Movie 2). Indeed, clusters in control follicles have

just one protrusion in 64% of the frames analyzed, whereas this is strikingly reduced to 34% of the frames in *fascin*-null follicles (Figure 8C). Furthermore, the clusters in *fascin*-null follicles have a higher percentage of frames with 3-4 protrusions (19%) compared to those of controls (1%) (Figure 8C;  $p<0.0001$ , Pearson's chi-squared test). Moreover, we assessed the localization of the protrusions to the front ( $0^\circ$  to  $45^\circ$  and  $0^\circ$  to  $315^\circ$ ), sides ( $45^\circ$  to  $135^\circ$  and  $225^\circ$  to  $315^\circ$ ), or back ( $135^\circ$  to  $225^\circ$ ) of the cluster.<sup>35</sup> Clusters in *fascin*-null follicles have significantly altered protrusion localization with 43% of the protrusions emerging from either the side or back of the cluster compared to 17% for the control clusters (Figure 8D;  $p<0.0001$ , Pearson's chi-squared test).

In addition, we measured protrusion length and binned them based on their directionality in the same manner as described above. The protrusions that emerge from the front of the cluster are typically longest in length.<sup>22,34</sup> Protrusions extending from the front of the cluster are significantly longer in control follicles compared to those in *fascin* mutant follicles (Figure 8E;  $9.3\mu\text{m}$  compared to  $7.5\mu\text{m}$ , respectively,  $p=0.045$ ). In control follicles, the protrusions extending from the front are significantly longer than the protrusions extending from the sides (Figure 8E; front= $9.3\mu\text{m}$ , sides= $6.6\mu\text{m}$ ,  $p=0.047$ ). Conversely, clusters in *fascin*-null follicles extend protrusions of similar lengths from all sides of the cluster (Figure 8E; front= $7.5\mu\text{m}$ , sides= $6.8\mu\text{m}$ , and back= $7.2\mu\text{m}$ ). Additionally, protrusion duration is significantly shorter in the *fascin*-null follicles, with the average duration being 20min compared to 43.4min for controls (Figure 8F,  $p<0.0001$ ).

Lastly, we quantified the migration speed of clusters during the first half of the migration; note that only fully delaminated clusters were assessed. Loss of Fascin results in significantly slower migration ( $0.26\mu\text{m}/\text{min}$ ) compared to controls ( $0.50\mu\text{m}/\text{min}$ ; Figure 8G;  $p=0.0085$ ). Overall, these data indicate that loss of Fascin impairs protrusion formation and regulation within the cluster, and these impairments cause slower migration speeds.

### Fascin regulates the delamination of the border cells

In addition to regulating protrusions during migration, we find Fascin also contributes to border cell delamination. Delamination is the process by which the border cell cluster detaches from the surrounding follicle cells to begin its migration. Live-imaging of follicles during delamination revealed in *fascin*-null follicles the border cell clusters spend more time detaching from the follicular epithelium (Figure 9B-B'' and Movie 4 compared to 9A-A'' and Movie 3). We quantified this change in delamination time by measuring the amount of time elapsed from cluster formation to when the cluster is fully delaminated during early S9. The clusters in *fascin*-null follicles take over two times longer to delaminate (301min) compared to control clusters (147min, Figure 9C; p<0.0001). Additionally, 3 clusters in *fascin*-null follicles failed to delaminate during the course of imaging; this high incidence of failure to delaminate seen by live imaging is likely due to the *in vitro* conditions not fully recapitulating the *in vivo* environment, resulting in an increased severity of the defects. To confirm the delamination defects seen in the *fascin*-mutants aren't solely caused by live imaging, we quantified the percentage of clusters that displayed delayed delamination from our previous fixed image analyses (Figure 2). Since the average diameter of the border cell clusters is approximately 25-35 $\mu$ m, we defined a cluster as having not delaminated if the border cell distance was less than 30 $\mu$ m. The *fascin*-null follicles have a significant increase in the percentage of clusters that haven't delaminated compared to wild-type or *fascin* heterozygous follicles (Figure 9D, p<0.001). Together these data indicate Fascin promotes border cell delamination.

While this delamination defect may be caused by the impaired cluster protrusions in *fascin* mutant follicles (Figure 8), another critical regulator of delamination is cellular adhesions. Disassembly of cell-cell adhesions between border cells and neighboring follicle and nurse cells is critical for proper delamination.<sup>21,36,37</sup> One adhesion molecule that must be regulated is E-Cadherin (*Drosophila* Shotgun).<sup>21,36</sup> Increasing or decreasing E-Cadherin in the border cells or nurse cells leads to defects in border cell migration.<sup>21,37</sup> As loss of Fascin is seen to increase E-Cadherin in hepatocellular carcinoma cells<sup>38</sup>, we hypothesized that Fascin and E-Cadherin may interact in this way during border cell migration. We were unable to test this hypothesis by

assessing dominant genetic interactions between *e-cadherin* and *fascin* mutants because heterozygosity for mutations in *e-cadherin* resulted in border cell migration delays during S9 (data not shown). Therefore, we assessed E-Cadherin by immunofluorescence and stained wild-type and *fascin* mutant follicles in the same tube to account for potential staining variability. We observe increased E-Cadherin membrane staining throughout the S9 follicle in *fascin*-null follicles. Notably, we observe a significant increase in the E-Cadherin at the nurse cell-nurse cell boundaries (Figure 10A-C). As expected, delaminating border cell clusters in control follicles have intense E-Cadherin staining at the border cell-polar cell boundary and lower intensity staining at the cluster periphery (border cell-nurse cell boundary, Figure 10E-E'). However, in *fascin*-null follicles the delaminating clusters have altered E-Cadherin localization, with a stronger intensity of staining at the cluster periphery (border cell-nurse cell boundary, Figure 10F-F'). These differences were analyzed by intensity labeling (Figure 10F' compared to E', yellow arrowheads), line-scan analysis (Figure 10H compared to G) and quantifying the relative fluorescence intensity of E-Cadherin at the cluster periphery normalized to phalloidin at the same location (Figure 10D). By all of these approaches, we observe a significant increase in the amount of E-Cadherin at the cluster periphery in *fascin*-null follicles (Figure 10D-H). These results suggest that Fascin is required for regulating E-Cadherin levels on the membranes of both the nurse cells and the delaminating border cell clusters. We speculate this increased E-Cadherin may impede border cell delamination.

## Discussion

Here we provide evidence that Fascin regulates invasive, collective cell migration. Specifically, Fascin is required for on-time border cell migration during S9 of *Drosophila* oogenesis (Figure 2). Using a new method to assess border cell migration during S9 (Figure 1), we find that Fascin functions not only within the border cells, but also in the nurse cells, the substrate on which the border cells migrate, to mediate on-time migration (Figures 3-6). Further, Fascin genetically interacts with Ena, an actin elongation factor, to mediate border cell migration

(Figure 7). Additionally, live imaging uncovered that Fascin regulates border cell cluster protrusions (Figure 8). These data, in conjunction with prior studies<sup>9,12</sup>, lead us to speculate that the actin bundling function of Fascin promotes the actin elongation activity of Ena within the border cells to mediate protrusion dynamics necessary for on-time border cell migration. Additionally, loss of Fascin impairs border cell delamination (Figure 9), which may be the result of impaired protrusion formation (Figure 8) that aids in pulling the cluster away from the epithelium and/or altered E-Cadherin localization in the delaminating cluster and surrounding nurse cells (Figure 10). Ultimately, our findings reveal that Fascin has multiple roles in regulating the invasive, collective border cell migration.

While studies on border cell migration have previously focused on whether the migration is completed by S10A of oogenesis, here we use a new method to quantitatively assesses border cell migration during S9 (Figure 1).<sup>39</sup> This method allows for the identification of factors that function in migration but don't cause a failure to complete migration by S10. These factors may play important roles in the migration process and/or control specific aspects of the migration that lead to delays, rather than impairing it as a whole. Additionally, the method can be used to identify factors that accelerate collective migration. Identifying and defining the roles of all the factors contributing to border cell migration, including the ones that only alter migration during S9, is essential to fully understanding the process of collective, invasive cell migration not only in *Drosophila* but in other systems.

Subtle changes in rates of collective migration can have large impacts, including during wound healing and cancer metastasis. For example, even if wounds close in the same overall time, delays in early wound healing can lead to complications, such as infection.<sup>40</sup> Thus, understanding the factors that control such delays provides key insight into the migration process and avoiding wound complications. Additionally, multiple factors likely influence invasive, collective migrations, such as cancer metastasis, and understanding where and how each factor influences the migration may lead to improved therapeutic interventions.<sup>41</sup> Overall, defects in

invasive, collective cell migration can stem from complete failure to migrate or delays in migration, however both have physiological consequences.

We find that loss of Fascin results in delayed border cell migration during S9, yet the migration is completed by S10A. The physiologic relevance of this delayed border cell migration in the robust system of *Drosophila* oogenesis is unclear. We find that knockdown of Fascin with the *c355* GAL4 or the *c306* GAL4 results in reduced fertility (Figure 4G). We hypothesize that this decrease in fertility is due to knocking down Fascin in the border cells and causing delayed migration. This hypothesis is based on the limited overlap of Fascin and the *c306* GAL4 expression patterns<sup>30,31</sup> Indeed, throughout oogenesis Fascin expression is largely restricted to the nurse cells. In the somatic cells, Fascin is extremely weakly expressed in the follicle cells, with the exception that it is highly expressed in the border cells and a few posterior follicle cells (Figure 4A).<sup>25</sup> The *c306* GAL4 is expressed in the follicle stem cells, stalk cells, and a group of anterior and posterior follicle cells, including the border cells. Thus, the expression of the *c306* GAL4 and Fascin primarily overlap in the border cells and some posterior follicle cells. As *fascin*-null mutants do not exhibit any posterior patterning defects, any defects resulting from RNAi knockdown of Fascin with the *c306* GAL4 driver are likely to be caused by issues with the border cells. Therefore, the delayed border cell migration observed by RNAi knockdown of Fascin with *c306* GAL4 is presumed to be due to knockdown within the border cells. Further, we speculate that delayed border cell migration during S9 causes defects in follicle development that decrease fertility.

We find that on-time S9 border cell migration requires Fascin in multiple cell types. Fascin functions within the somatic cells, specifically the border cells, as knockdown of Fascin in these cells delays migration and expression of Fascin in the border cells restores migration in *fascin* mutants (Figure 3-5). Additionally, Fascin acts within the germline cells, the substrate on which the border cells migrate, as germline knockdown of Fascin causes migration delays (Figure 3). However, germline expression of Fascin didn't rescue migration in *fascin* mutants (Figure 5). We speculate this failure to rescue is caused by the strong overexpression of Fascin in

the nurse cells causing significant morphological defects in the border cell cluster that likely impede migration (Figure 6). These findings suggest that Fascin level or activity must be tightly regulated in the nurse cells. Together these data indicate Fascin is required in both the border cells and the nurse cells for on-time border cell migration.

Surprisingly, restoring Fascin expression in the somatic or border cells of *fascin* mutants (Figure 5) and knockdown of Fascin in the germline cells (Figure 3) cause opposing phenotypes in border cell migration. While we still don't understand the cause for these differences, there are numerous ways in which we speculate this may occur. For example, the balance of forces between the nurse cells and border cells is important for border cell migration.<sup>27</sup> This balance may be differentially affected in the somatic rescue compared to the germline knockdown of Fascin, leading to the distinct effects on border cell migration. Alternatively, Fascin expression in the somatic rescue may be at a higher level than endogenous expression and this may bypass endogenous regulation, permitting increased Fascin activity in the somatic cells that overcomes the need for germline Fascin. Additionally, there may be signaling and communication between the border cells and nurse cells that is needed for proper migration. Severe reduction of Fascin in either cell-type could perturb this signaling enough to inhibit border cell migration, whereas restoring expression in the border cells may be sufficient to restore the signaling to promote on-time migration. Further investigation is warranted to understand the cell-specific roles of Fascin in mediating on-time border cell migration.

We hypothesize that Fascin regulates the stiffness of the nurse cells which must be tightly regulated for on-time border cell migration. Supporting this idea, overexpression of Fascin in the germline results in abnormal cluster morphology (Figure 6), while RNAi knockdown in the germline causes delayed migration (Figure 3). A means by which Fascin may alter nurse cell stiffness is by controlling nurse cell-nurse cell adhesion. Indeed, E-Cadherin levels are higher on all cell membranes, including the nurse cells during S9 in *fascin*-null mutants (Figure 10A-C). Such increased adhesion can impede border cell migration.<sup>21</sup> Also, increasing nurse cell stiffness by enhancing non-muscle myosin II contractility impairs border cell migration.<sup>27,28</sup> Interestingly,

*in vitro* Fascin inhibits non-muscle myosin II.<sup>42</sup> Therefore, loss of Fascin in the nurse cells may increase non-muscle myosin II contractility, resulting in stiffer nurse cells and delayed border cell migration. Finally, Fascin may regulate the structure of the cortical actin in the nurse cells to control stiffness, as loss of Fascin results in cortical actin breakdown during mid-oogenesis.<sup>43</sup> Further studies are needed to understand how Fascin functions within the germline to modulate border cell migration.

One way by which Fascin may contribute to border cell migration is by regulating the actin elongation factor, Ena. Our dominant genetic interaction studies indicate that Fascin and Ena work within the same pathway to regulate border cell migration (Figure 7A-C). Additionally, overexpression of Ena in the somatic cells restores border cell migration in *fascin* mutants (Figure 7D-F). Together these data indicate that Fascin acts upstream of Ena to promote border cell migration. As previous *in vitro* studies uncovered that Ena has increased processivity on actin bundled specifically by Fascin<sup>9,12</sup>, we speculate that Fascin acts to increase Ena processivity to promote protrusion formation necessary for mediating on-time border cell migration.

Border cell protrusion formation and dynamics are regulated by Fascin. Loss of Fascin results in shorter and mislocalized protrusions (Figure 8C-E). Consistent with this finding, in both *Drosophila* and cancer cells loss of Fascin results in shorter protrusions during single cell migration.<sup>3,44</sup> Border cell protrusion duration is also shorter in clusters of *fascin*-null follicles (Figure 8F). This observation is consistent with the finding that Fascin contributes to protrusion persistence by stabilizing actin bundles.<sup>45</sup> While germline Fascin may have a role in regulating cluster protrusions, these data, along with the delayed migration when Fascin is knocked down in the border cells and somatic Ena rescue of the delayed migration in the *fascin* mutants, favors the model that Fascin functions within the border cells to regulate protrusions.

Fascin also regulates the delamination of the border cell cluster. Loss of Fascin results in significantly longer delamination times by live imaging (Figure 9). This finding is supported by analysis of our fixed imaging data, which reveals ~16% of the border cell clusters in *fascin*-null

follicles exhibit delayed delamination. Thus, we observe delays in delamination using both fixed and live imaging. Additionally, we find using live imaging that fully delaminated clusters of *fascin*-null follicles migrate significantly slower during mid-migration. These results indicate that the delays we see in on-time border cell migration in the *fascin*-null follicles come from a combination of both slower migration speeds and delays in delamination. Contributing to this delamination defect could be the impaired protrusion formation of the cluster (Figure 8) and/or retention of high levels of E-Cadherin on the membranes at the border cell-nurse cell boundaries and/or between the nurse cells (Figure 10). Proper levels of E-Cadherin between both the nurse cells and border cells are necessary for migration, as knockdown or overexpression of E-Cadherin in the border cells or nurse cells results in impaired border cell migration.<sup>21,37</sup> Therefore, persistence of E-Cadherin along these boundaries may impair border cell delamination. Notably, knockdown of Fascin increases E-Cadherin in hepatocellular carcinoma cells.<sup>38</sup> These findings lead us to hypothesize that Fascin regulates E-Cadherin localization or stabilization during *Drosophila* oogenesis in a similar manner.

Fascin activity must be tightly regulated to ensure proper cell migration. One of the ways that Fascin is regulated is through phosphorylation.<sup>3,8,46</sup> PKC phosphorylates Fascin and following this phosphorylation Fascin cannot bundle actin.<sup>8</sup> Additionally, phosphorylated Fascin interacts with PKC<sup>46</sup> and disruption of this interaction increases cellular protrusions.<sup>8</sup> Moreover, atypical PKC zeta regulates border cell migration<sup>47</sup>, but it is unclear if other forms of PKC also do this. Future studies are needed to determine if phosphorylation regulates Fascin during border cell migration. Additionally, previous work in our lab demonstrated that Fascin is regulated by prostaglandins (PGs).<sup>43</sup> PGs are lipid signaling molecules that mediate a wide variety of biological processes, including cytoskeletal dynamics.<sup>48-51</sup> Our lab previously showed that PGs regulate actin bundling during *Drosophila* oogenesis through Fascin.<sup>43</sup> Additionally, we find that PGs are required for on-time border cell migration and regulate Fascin in this context as well.<sup>39</sup> Exactly how PGs control Fascin has yet to be determined, however this may occur through regulating Fascin phosphorylation (Groen and Tootle, unpublished data) and/or localization.<sup>7,52</sup>

In addition to regulating Fascin, PGs also regulate the localization and activity of Ena in the nurse cells.<sup>53</sup> As described above, we speculate that Fascin regulates Ena processivity during border cell migration; these findings suggest that PGs may modulate the interaction between Fascin and Ena. Thus, PGs may regulate multiple functions of Fascin to control border cell migration. Altogether, future studies are needed to define the means regulating Fascin during border cell migration.

Border cell migration recapitulates the collective cell migration often seen during cancer metastasis and enables one to study essential aspects of this migration, such as cluster adhesion or polarization.<sup>20,54</sup> Fascin's role in promoting cancer metastasis is well documented in several types of carcinomas.<sup>2,55</sup> Fascin is not typically expressed in adult epithelial tissues, however elevated expression of Fascin in epithelial cancers has been correlated with increased aggressiveness, mortality, and notably, metastasis.<sup>2,17,56</sup> In fact, knockdown of Fascin decreases metastasis in a xenograft tumor model of colon cancer.<sup>10</sup> Here we identified Fascin as a new regulator of border cell migration and find that Fascin influences both protrusion and adhesion dynamics to control on-time S9 migration. Thus, border cell migration is a simplified, *in vivo*, and genetic tractable system to define the roles of Fascin in regulating invasive, collective cell migration.

## Experimental Procedures:

### Fly stocks

Fly stocks were maintained on cornmeal/agar/yeast food at 21°C, except where noted. Before immunofluorescence and live imaging, flies were fed wet yeast paste daily for 2-4 days. Unless otherwise noted, *yw* was used as the wild-type control. The following stocks were obtained from the Bloomington Stock Center (Bloomington, IN): *sn<sup>X2</sup>*, *ena<sup>210</sup>*, *ena<sup>23</sup>*, *matα* GAL4 (third chromosome), *c355* GAL4, *c306* GAL4, *actin5C* GAL4, and *UASp-RNAi-Fascin* (TRiP.HMS02450 and TRiP.HMJ21813). The *sn28* line was a generous gift from Jennifer Zanet (Université de Toulouse, Toulouse, France)<sup>3</sup>, the *oskar* GAL4 line (second chromosome) was a

generous gift from Anne Ephrussi (European Molecular Biology Laboratory, Heidelberg, Germany)<sup>57</sup>, the *UASp-GFP-Fascin* wild-type transgenic fly line was a generous gift from Francois Payre (Université de Toulouse, Toulouse, France)<sup>58</sup>, the *UASp-RFP-Ena* wild-type transgenic fly line was a generous gift from Mark Peifer (University of North Carolina, Chapel Hill, NC, unpublished) and the *slbo>mCD8-GFP* transgenic fly line was a generous gift from Xiaobo Wang (French National Centre for Scientific Research, Toulouse, France, unpublished). For germline expression during S9, either *mat $\alpha$*  GAL4 or *oskar* GAL4 can be utilized interchangeably. Expression of *UASp-RNAi-Fascin* was achieved by crossing to *mat $\alpha$*  GAL4, *c355* GAL4, and *c306* GAL4, and maintaining crosses at 25°C and progeny at 29°C. The *sn28*, *c355* GAL4 flies were generated by recombining *sn28* and *c355* GAL4 onto the same chromosome. Briefly, *sn28*, *c355* GAL4 males were identified by selecting for the *singed* phenotype (marker for *sn28*) and *w<sup>+</sup>* eyes (marker for *c355* GAL4). Recombination was verified by crossing *sn28*, *c355* GAL4/FM7 flies to *sn28*; *UASp-GFP-Fascin* and assessing both GFP expression and *singed* phenotype. A similar recombination scheme was performed to generate *sn28*, *c306* GAL4/FM7 flies. Expression of *UASp-GFP-Fascin* was achieved by crossing to *oskar* GAL4, *c355* GAL4, and *actin5C* GAL4, and maintaining crosses at 25°C and progeny at 29°C. Expression of *UASp-RFP-Ena* was achieved by crossing to *sn28*, *c355* GAL4, and maintaining crosses at 25°C and progeny at 29°C.

### Fertility Assays

Three females (3 or 4 days old, fed wet yeast every day prior to mating) of the indicated genotypes were maintained at 29°C and allowed to mate with two to three wild-type (*yw*) males for 2 days. Matings were performed in triplicate for each genotype. Fresh wet yeast was provided daily. The flies were then transferred to a fresh vial, provided wet yeast, and allowed to lay eggs for 24 h. The adults were removed after 24 h, the vial containing the laid eggs was maintained at room temperature, and the resulting adult progeny were counted ~18 days later. The number of

progeny per female was determined for each vial of the three independent vials per genotype. Statistical analysis was performed using Prism (Graphpad Software, LaJolla, CA).

### Immunofluorescence

Whole-mount *Drosophila* ovary samples (approximately 5 flies per experiment) were dissected into Grace's insect media and fixed for 10 minutes at room temperature in 4% paraformaldehyde in Grace's insect media (Lonza, Walkersville, MD or Thermo Fischer Scientific, Waltham, MA). Briefly, samples were blocked using Triton antibody wash (1X phosphate-buffered saline, 0.1% Triton X-100, and 0.1% bovine serum albumin) six times for 10 minutes each. Primary antibodies were diluted with Triton antibody wash and incubated overnight at 4°C. The following primary antibodies were obtained from the Developmental Studies Hybridoma Bank (DSHB) developed under the auspices of the National Institute of Child Health and Human Development and maintained by the Department of Biology, University of Iowa (Iowa City, IA): mouse anti-Hts 1:50 (1B1, Lipshitz, HD)<sup>59</sup>, mouse anti-FasIII 1:50 (7G10, Goodman, C)<sup>60</sup>, mouse anti-Fascin 1:20 (sn7c, Cooley, L)<sup>25</sup>, and rat anti-DCAD2 1:20 (Umemura, T)<sup>61</sup>. Additionally, the following primary antibody was used: rabbit anti-GFP 1:2000 (pre-absorbed on yw ovaries at 1:20 and used at 1:100; Torrey Pines Biolabs, Inc., Secaucus, NJ) and rabbit anti-dsRed 1:300 (Clontech, Mountain View, CA). After 6 washes in Triton antibody wash (10 minutes each), secondary antibodies were incubated overnight at 4°C or for ~4 hours at room temperature. The following secondary antibodies were used at 1:500: AlexaFluor (AF)488::goat anti-mouse, AF568::goat anti-mouse, AF488::goat anti-rabbit, AF568::goat anti-rabbit (Thermo Fischer Scientific) and AF647::goat anti-mouse and AF488::goat anti-rat (Jackson ImmunoResearch Laboratories, Inc., West Grove, PA). AF647-, rhodamine, or AF568-conjugated phalloidin (Thermo Fischer Scientific) was included with primary and secondary antibodies at a concentration of 1:250. After 6 washes in Triton antibody wash (10 minutes each), 4',6-diamidino-2-phenylindole (5 mg/ml) staining was performed at a concentration of 1:5000 in 1X PBS for 10 minutes at room temperature. Ovaries were mounted in 1 mg/ml

phenylenediamine in 50% glycerol, pH 9.<sup>62</sup> All experiments were performed a minimum of three independent times.

### **Image acquisition and processing**

Microscope images of fixed *Drosophila* follicles were obtained using LAS AS SPE Core software on a Leica TCS SPE mounted on a Leica DM2500 using an ACS APO 20x/0.60 IMM CORR -D objective (Leica Microsystems, Buffalo Grove, IL) or using Zen software on a Zeiss 700 LSM mounted on an Axio Observer.Z1 using a Plan-APOCHROMAT 20x/0.8 working distance (WD) = 0.55 M27 or a EC-Plan-Neo-Fluar 40x/1.3 oil objective (Carl Zeiss Microscopy, Thornwood, NY). Maximum projections (two to four confocal slices), merged images, rotations, and cropping were performed using ImageJ software.<sup>63</sup> S9 follicles were identified during fixed imaging by the size of the follicle (~150-250 $\mu$ m), the position and morphology of the outer follicle cells, and presence of a border cell cluster. The beginning of S10 was defined as when the anterior most outer follicle cells reached the nurse cell-oocyte boundary and flattened.

### **Quantification of fixed imaging**

Quantification of the migration index of border cell migration during S9 was performed on confocal image stacks of follicles stained with anti-Hts and anti-FasIII or phalloidin. Measurements of migration distances were obtained from maximum projections of 2-4 confocal slices of deidentified 20x confocal images using ImageJ software.<sup>63</sup> Briefly, a line segment was drawn from the anterior end of the follicle to the front or posterior of the border cell cluster and the distance in microns measured; this was defined as the distance of border cell migration. Additionally, a line segment was drawn from the anterior end of the follicle to the anterior end of the main-body follicle cells and the distance measured; this was defined as the distance of the outer follicle cells. Lastly, the entire follicle length was measured along the anterior-posterior axis. The migration index was calculated in Excel (Microsoft, Redmond, WA) by dividing the border cell distance by the follicle cell distance. For the border cell knockdown of Fascin in

Figure 4, we only quantified S9 follicles that had sufficient Fascin knockdown in the border cells. A sufficient knockdown of Fascin in the border cell cluster was defined as a cluster that had similar or lower Fascin staining than the surrounding nurse cells. To demonstrate there are no changes in outer follicle cell morphogenesis, the follicle length versus outer follicle cell distance was plotted and linear regression lines generated in Prism (GraphPad Software). For border cell cluster size, the area was measured on 20x images in a genotypically blinded manner in ImageJ by tracing the outline of the border cell cluster from the center confocal slice of the cluster. For the analysis of delamination using fixed imaging, a border cell cluster was defined as not yet delaminated if the distance of border cell migration was less than 30 $\mu$ m. The percent of clusters with delayed delamination was calculated for each genotype. All analyses were done in a genotypically blinded manner. Data was compiled, graphs generated, and statistical analysis performed using Prism (GraphPad Software).

### **Line scan and intensity analysis of E-Cadherin**

Line scan and intensity analysis were performed on maximum projections of 2 confocal slices of a 40x confocal image using ImageJ software.<sup>63</sup> For the line scan analysis, briefly, a line segment was drawn across a delaminating border cell cluster and the plot profile function was used to generate a fluorescence intensity plot for E-Cadherin these values were then normalized to the phalloidin intensity along the same line. Raw data was graphed in Prism (GraphPad Software). The cell boundaries were defined as the peaks in fluorescence intensity. For E-Cadherin intensity analysis, 3 line segments per follicle were drawn across nurse cell-nurse cell membranes and border cell-nurse cell boundaries on maximum projections of 2-3 confocal slices of *wild-type* and *fascin*-null follicles stained for E-Cadherin and phalloidin. The fluorescent intensity peak for E-Cadherin was determined for each line and normalized to phalloidin intensity at the same point. These three values were then averaged for a single image. Data was compiled, graphs generated, and statistical analysis performed using Prism (GraphPad Software). To aid in visualization E-

Cadherin and phalloidin images were all brightened by 40% in Photoshop (Adobe, San Jose, CA).

### Live imaging

Whole ovaries were dissected from flies fed wet yeast past for 2-3 days and maintained at 25°C until the last 16-24 hours when they were moved to 29°C. Genotypes used for live imaging were *sn28/FM7; slbo>mCD8-GFP* and *sn28/sn28; slbo>mCD8-GFP*. Ovaries were dissected in Stage 9 (S9) medium (Prasad *et al.* 2007): Schneider's medium (Life Technologies), 0.6x penicillin/streptomycin (Life Technologies). 0.2 mg/ml insulin (Sigma-Aldrich, St. Louis, MO), and 15% fetal bovine serum (Atlanta Biologicals, Flowery Branch, GA). S9 follicles were hand dissected and embedded in 1.25% low-melt agarose (IBI Scientific, Peosta, IA) made with S9 media on a coverslip-bottom dish (MatTek, Ashland, MA). Just prior to live imaging, fresh S9 media was added to coverslip-bottom dish. Live imaging was performed with Zen software on a Zeiss 700 LSM mounted on an Axio Observer.Z1 using a Plan-Apochromat 20x/0.8 working distance (WD) = 0.55 M27 (Carl Zeiss Microscopy, Thornwood, NY). Images were acquired every 5-5.5 mins for at least 3 hours. Maximum projections (2-5 confocal slices), merge images, rotations, and cropping were performed using ImageJ software.<sup>63</sup> To aid in visualization live imaging videos and stills were inverted in ImageJ and brightened by 50% in Photoshop (Adobe, San Jose, CA).

### Quantification of live imaging

Quantification of live imaging videos was based on analyses done in Sawant *et al.*<sup>35</sup> Analyses were performed in ImageJ<sup>63</sup> using maximum projection of 2-5 confocal slices from time-lapse videos of border cell migration. Parameters quantified include number of protrusions per frame, protrusion length, protrusion duration, and migration speed. For number of protrusions per frame, the number of protrusions emerging from the front (0° to 45° and 0° to 315°), sides (45° to 135° and 225° to 315°), and back (135° to 225°) of the cluster was counted per frame for an

hour of migration. For protrusion length and number, a protrusion was defined as an extension longer than 4  $\mu\text{m}$  from the cluster body. The length of the protrusions was measured and binned into groups based on the direction emerging from cluster: front ( $0^\circ$  to  $45^\circ$  and  $0^\circ$  to  $315^\circ$ ), sides ( $45^\circ$  to  $135^\circ$  and  $225^\circ$  to  $315^\circ$ ), and back ( $135^\circ$  to  $225^\circ$ ). Protrusion duration was measured by quantifying the amount of time elapsed between the very beginning of extension and the protrusion fully retracting for protrusions that were greater than 4  $\mu\text{m}$  at their maximum length. Migration speed was calculated during the first half of migration for approximately an hour by measuring cluster displacement dividing by time elapsed. For delaminating clusters, delamination time was defined as the amount of time elapsed from early S9 to when the border cell cluster completely detached from the epithelium. Data was compiled, graphs generated, and statistical analysis performed using Prism (GraphPad Software).

### Acknowledgements

We thank the Westside Fly Group and Dunnwald lab for helpful discussions and the Tootle lab for helpful discussions and careful review of the manuscript. We thank Xiaobo Wang for the *slbo>mCD8-GFP* fly stock. Stocks obtained from the Bloomington Drosophila Stock Center (NIH P40OD018537) were used in this study. Information Technology Services – Research Services provided data storage support. This project is supported by National Institutes of Health R01GM116885. M.C.L. is partially supported by the University of Iowa Summer Graduate Fellowship and has previously been supported by the Anatomy and Cell Biology Department Graduate Fellowship.

### Figure legends:

**Figure 1: Quantification of border cell migration during Stage 9.** (A) Schematic of follicle development and the migration index quantification for border cell migration during S9. The migration index is the distance the border cell cluster has migrated divided by the distance of the

outer follicle cells from the anterior end. A value of ~1 indicates on-time migration, a value <1 indicates delayed migration and a value >1 indicates accelerated migration. **(B-C)** Maximum projections of 2-4 confocal slices of S9 follicles of the indicated genotypes. Hts/FasIII (border cell stain)=white. Blue lines indicate distance of border cells measured in microns and orange lines indicate distance of outer follicle cells measure in microns. Below is an example calculation of migration index for each follicle. Scale bars = 50 $\mu$ m. **(B)** wild-type. **(C)** *fascin*<sup>sn28/sn28</sup>. Follicles grow in size and border cell migration occurs throughout S9, and the migration index quantifies changes in this migration.

**Figure 2: Fascin is required for on-time border cell migration.** **(A-C)** Maximum projections of 2-4 confocal slices of S9 follicles of the indicated genotypes. Merged images: Hts/FasIII (white, border cell migration stain), phalloidin (magenta), and DAPI (cyan). Yellow lines=outer follicle cell distance. Yellow arrows=border cell cluster. Black boxes added behind text. Scale bars=50 $\mu$ m. **(A)** wild-type (*yw*). **(B)** *fascin*<sup>sn28/+</sup>. **(C)** *fascin*<sup>sn28/sn28</sup>. **(D, F)** Migration index quantification of the indicated genotypes. In F, follicles are binned into groups based on overall follicle length. Dotted line at 1=on-time migration. Circle=S9 follicle. Lines=averages and error bars=SD. n=# of follicles, \*p<0.05, \*\*\*p<0.001, \*\*\*\*p<0.0001 (D: One-way ANOVA with Tukey's multiple comparison test; F: Student's t-test). **(E)** Graph of follicle length versus outer follicle cell distance for wild-type (black open circles) and *fascin*<sup>sn28/sn28</sup> (blue circles) S9 follicles. Loss of Fascin results in significant border cell migration delays during S9 (C-D compared to A-B). The follicle cell distance vs follicle length is similar between wild-type and *fascin*-null follicles, indicating outer follicle cell morphogenesis is not altered in *fascin* mutant follicles (E) and significant migration index delays are observed throughout S9 in *fascin*-null follicles (F).

**Figure 3: Fascin is necessary in both the somatic and germline cells for on-time border cell migration.** **(A-D)** Maximum projections of 2-4 confocal slices of S9 follicles of the indicated

genotypes. Merged images: Hts/FasIII (white, border cell migration stain), phalloidin (magenta), and DAPI (cyan). Yellow lines=outer follicle cell distance. Yellow arrows=border cell cluster. Black boxes added behind text. Scale bars=50 $\mu$ m. **(A)** RNAi only (*fascin RNAi/+*). **(B)** Germline knockdown of Fascin (*mat $\alpha$  GAL4(3)/fascin RNAi*). **(C)** Somatic cell knockdown of Fascin (*c355 GAL4/+; +/fascin RNAi*). **(D)** Border cell knockdown of Fascin (*c306 GAL4/+; +/fascin RNAi*). **(E)** Migration index quantification of the indicated genotypes. Dotted line at 1=on-time migration. Circle=S9 follicle. Lines=averages and error bars=SD. n=# of follicles. p-values indicated on graph (One-way ANOVA with Tukey's multiple comparison test). Fascin is necessary for on-time border cell migration in both the germline (B, E) and somatic cells (C, E), specifically the border cells (D, E).

**Figure 4: Fascin is necessary in border cells for on-time migration and female fertility. (A-E)** Maximum projections of 2-4 confocal slices of S9 follicles of the indicated genotypes. (A-C) Fascin (white). (A'-C', D-E) Merged images: Fascin (magenta), phalloidin (white), and DAPI (cyan). Yellow lines=outer follicle cell distance. Yellow arrows=border cell cluster. Black boxes added behind text. Scale bars=50 $\mu$ m. **(A-A')**, **(D)** RNAi only (*fascin RNAi/+*). **(B-B')** Border cell KD of Fascin (*c306 GAL4/+; +/fascin RNAi*) in early S9. **(C-C')**, **(E)** Border cell KD of Fascin (*c306 GAL4/+; +/fascin RNAi*) in mid-to-late S9. **(F)** Migration index quantification of the indicated genotypes. Dotted line at 1=on-time migration. Circle=S9 follicle. Lines=averages and error bars=SD. n=# of follicles. \*\*\*\*p<0.0001 (One-way ANOVA with Tukey's multiple comparison). **(G)** Graph of average number of adult progeny/female of the indicated genotypes from a 24 hour egg-lay. Circle=average progeny/female of 3 females. Error bars=SD. \*p<0.05, \*\*\*p<0.001 (One-way ANOVA with Tukey's multiple comparison). While knockdown of Fascin in the border cells is variable (B-C'), assessment of successful knockdown reveals Fascin is required in the border cells for on-time migration (D-F). Knockdown of Fascin in the germline, somatic or border cells results in decreased female fertility (G).

**Figure 5: Somatic and border cell expression of Fascin rescues border cell migration. (A-H)**  
Maximum projections of 2-4 confocal slices of S9 follicles of the indicated genotypes. Merged images: Hts/FasIII (white, border cell migration stain), GFP (magenta), and DAPI (cyan). Yellow lines=outer follicle cell distance. Yellow arrows=border cell cluster. Black boxes added behind text. Scale bars=50 $\mu$ m. (A) *fascin* mutant with somatic GAL4 (*c355 GAL4, fascin<sup>sn28</sup>/fascin<sup>sn28</sup>*). (B) Somatic GFP-Fascin expression in *fascin* mutant (*c355 GAL4, fascin<sup>sn28/sn28</sup>; +/UAS-GFP-Fascin*). (C) *fascin* mutant with border cell GAL4 (*c306 GAL4, fascin<sup>sn28</sup>/fascin<sup>sn28</sup>*). (D) Border cell GFP-Fascin expression in *fascin* mutant (*c306 GAL4, fascin<sup>sn28/sn28</sup>; +/UAS-GFP-Fascin*). (E) *fascin* mutant with germline GAL4 (*fascin<sup>sn28/sn28</sup>; oskar GAL4(2)/+*). (F) Germline GFP-Fascin expression in *fascin* mutant (*fascin<sup>sn28/sn28</sup>; oskar GAL4(2)/UAS-GFP-Fascin*). (G) *fascin* mutant with global GAL4 (*fascin<sup>sn28/sn28</sup>; actin5C GAL4/+*). (H) Global GFP-Fascin expression in *fascin* mutant (*fascin<sup>sn28/sn28</sup>; actin5C GAL4/UAS-GFP-Fascin*). (I) Migration index quantification of the indicated genotypes. '+' and '-' indicate the presence and absence, respectively, of Fascin and GFP-Fascin. Dotted line at 1=on-time migration. Circle=S9 follicle. Lines=averages and error bars=SD. n=# of follicles. ns indicates p>0.05, \*p<0.05, \*\*p<0.01, \*\*\*\*p<0.0001 (One-way ANOVA with Tukey's multiple comparison). Expression of Fascin in the somatic cells (A-B, I), border cells (C-D, I) or globally (G-I) in *fascin*-null follicles rescues border cell migration, whereas germline expression fails to rescue migration (E-F, I).

**Figure 6: Germline expression of GFP-Fascin alters border cell cluster morphology. (A-D)**  
Maximum projections of 2-4 confocal slices of S9 follicles of the indicated genotypes. Hts/FasIII (border cell stain, white) and dotted yellow line outlines the border cell cluster. Scale bars = 50 $\mu$ m. (A) Germline GAL4 control (*oskar GAL4(2)/+*). (B) Germline GFP-Fascin expression in wild-type background (*oskar GAL4(2)/UAS-GFP-Fascin*). (C) GFP-Fascin control in *fascin* mutant (*fascin<sup>sn28/sn28</sup>; +/UAS-GFP-Fascin*). (D) Germline GFP-Fascin expression in *fascin* mutant (*fascin<sup>sn28/sn28</sup>; oskar GAL4(2)/UAS-GFP-Fascin*). (E) Graph of the cluster area for the

indicated genotypes. '+' and '-' indicate the presence and absence, respectively, of Fascin and GFP-Fascin. Circle=S9 follicle. Lines=averages and error bars=SD. n=# of follicles. \*p<0.05, \*\*\*p<0.0001 (One-way ANOVA with Tukey's multiple comparison). Overexpression of Fascin in the germline causes increased cluster area (A-E).

**Figure 7: Fascin genetically interacts with Ena to regulate border cell migration. (A-B, D-E)** Maximum projections of 2-4 confocal slices of S9 follicles of the indicated genotypes. Merged images: (A-B) Hts/FasIII (white, border cell stain), phalloidin (magenta), and DAPI (cyan); (D-E) Hts/FasIII (white, border cell stain), RFP (magenta), and DAPI (cyan). Yellow lines=outer follicle cell distance. Yellow arrows=border cell cluster. Black boxes added behind text. Scale bars = 50 $\mu$ m. (A) *ena*<sup>210</sup>/+. (B) *fascin*<sup>sn28</sup>/+; *ena*<sup>210</sup>/+. (D) RFP-Ena control in *fascin* mutant (*fascin*<sup>sn28/sn28</sup>; +/*UAS-RFP-Ena*). (E) Somatic Ena expression in *fascin* mutant (*c355 GAL4, fascin*<sup>sn28/sn28</sup>; +/*UAS-RFP-Ena*). (C, F) Migration index quantification of the indicated genotypes. '+' and '-' indicate the presence and absence, respectively, of Fascin, RFP-Ena, and the GAL4. Dotted line at 1=on-time migration. Circle=S9 follicle. Lines=averages and error bars=SD. n= # of follicles, ns indicates p>0.05, \*p<0.05, \*\*p<0.01, \*\*\*p<0.0001 (One-way ANOVA with Tukey's multiple comparison). Double heterozygotes for mutations in *fascin* and *ena* exhibit significant delays in border cell migration (A-C). Overexpression of Ena in the somatic cells rescues border cell migration in *fascin*-null follicles (D-F).

**Figure 8: Fascin regulates protrusion dynamics during border cell migration. (A-B'')** Maximum projections of 2-4 inverted confocal slices from time-lapse imaging of *slbo>mCD8-GFP* expression in the indicated genotypes; scale bars=50 $\mu$ m. Direction of migration is to the right. Insets=zoom-ins of the border cell clusters, red arrowheads=protrusions, and scale bars=10 $\mu$ m. (A-A'') Control follicle (*fascin*<sup>sn28</sup>/+; Movie 1). (B-B'') *fascin*-null follicle (*fascin*<sup>sn28/sn28</sup>; Movie 2). (C-F) Graphs of protrusion dynamics for control (n=7) and *fascin*-null follicles (n=7). Error bars=SD. (C) Quantification of the total number of protrusions per frame binned into groups based on total number of protrusions: 0, 1, 2, 3, or 4. \*\*\*p<0.0001

(Pearson's chi-squared test). **(D-E)** Quantification of the percent of protrusions per frame (D) and protrusion length (E) based on if they emerged from the front ( $0^\circ$  to  $45^\circ$  and  $0^\circ$  to  $315^\circ$ , black), sides ( $45^\circ$  to  $135^\circ$  and  $225^\circ$  to  $315^\circ$ , grey), or back ( $135^\circ$  to  $225^\circ$ , white) of the cluster. In D, only frames with at least 1 protrusion were counted; \*\*\*\*p<0.0001 (Pearson's chi-squared test). In E, a protrusion was defined as an extension  $\geq 4\mu\text{m}$  long; ns indicates p>0.05, \*p<0.05 (One-way ANOVA with Tukey's multiple comparison). **(F)** Quantification of protrusion duration, the total time elapsed between the protrusion ( $\geq 4\mu\text{m}$ ) beginning to extend and fully retracting. \*\*\*\*p<0.0001 (unpaired t-test). **(G)** Quantification of migration speed, the cluster displacement over time during the first half of migration. n=5 for control and *fascin*-null follicles. \*\*p<0.01 (unpaired t-test). Loss of Fascin results in border cells clusters with more protrusions (C) that are mislocalized on the cluster (D) and significantly shorter in length (E) and duration (F) compared to control clusters. Loss of Fascin also results in slower migration speeds (G).

**Figure 9: Fascin regulates border cell delamination.** **(A-B'')** Maximum projection of 3 inverted confocal slices from time-lapse imaging of *slbo>mCD8-GFP* expression in the indicated genotypes. Direction of migration is to the right. Scale bars = $50\mu\text{m}$ . **(A-A'')** Control follicle (*fascin*<sup>sn28/+</sup>; Movie 3). **(B-B'')** *fascin*-null follicle (*fascin*<sup>sn28/sn28</sup>; Movie 4). **(C)** Quantification of time to delamination from time-lapse imaging for control (*fascin*<sup>sn28/+</sup>, n=6) and *fascin*-null (*fascin*<sup>sn28/sn28</sup>, n=8) follicles. Time to delamination was defined as the amount of time elapsed from early S9 to when the border cell cluster completely detached from the epithelium. Three additional *fascin*-null clusters failed to completely delaminate during imaging time (data not included on graph). \*\*\*p<0.001 (unpaired t-test). Error bars=SD. **(D)** Quantification of percentage of clusters with delayed delamination using fixed imaging for wild-type (*yw*), *fascin* heterozygotes (*fascin*<sup>+/−</sup>) and *fascin*-null (*fascin*<sup>−/−</sup>) follicles; data for all heterozygous and homozygous genotypes were combined. A cluster was considered not yet delaminated if the border cell distance migrated  $<30\mu\text{m}$ . \*\*\*p<0.001 (Fischer's exact test).

*fascin* mutant border cells clusters take significantly longer to delaminate (B-D) compared to the control clusters (A, C, D).

**Figure 10: Fascin regulates E-Cadherin on the nurse cells and delaminating border cell clusters. (A-B', E-F')** Maximum projections of 2-4 confocal slices of S9 follicles of the indicated genotypes. (A, B) E-Cadherin (white). (A', B') phalloidin (white). (E, F) E-Cadherin (white). (E', F') E-Cadherin pseudocolored with Rainbow RGB, red=highest intensity pixels. (A-A', E-E') wild-type (*yw*). (B-B', F-F') *fascin*-null (*fascin*<sup>sn28/sn28</sup>). Samples were stained in the same tube. In E-F, nc = nurse cell, bc = border cell, and pc = polar cell, and yellow lines=or line scan analysis. In E'-F', yellow arrowheads=E-Cadherin intensity differences at the border cell-nurse cell boundary. Scale bars=20 $\mu$ m in A-B' and 10 $\mu$ m E-F'. (C, D) Graphs of quantification of E-Cadherin intensity at the nurse cell-nurse cell (C) and border cell-nurse cell boundary (D) in wild-type or *fascin*-null follicles. Peak E-Cadherin intensity was quantified and normalized to phalloidin staining, three measurements were taken per follicle and averaged; dot=follicle. \*\*\*p<0.001, \*\*\*\*p<0.0001 (unpaired t-test with Welch's correction). Error bars=SD. (G, H) Fluorescence intensity plots of E-Cadherin normalized to phalloidin along the yellow lines across a single border cell cluster (E, F) of the indicated genotypes. X-axis: distance; Y-axis: E-Cadherin fluorescent intensity/phalloidin fluorescent intensity. (G) Wild-type follicle (*yw*). (H) *fascin*-null follicle (*fascin*<sup>sn28/sn28</sup>). nc:bc and bc:nc=nurse cell-border cell boundary (red). pc:bc and bc:pc=polar cell-border cell boundary (blue). The *fascin*-null follicles have increased E-Cadherin on the nurse cells (A-C) and the border cell cluster periphery (D-H) compared to wild-type follicles.

**Movie 1. Control border cell migration.** Inverted video of S9 control follicle (*fascin*<sup>sn28/+</sup>; *slbo>mCD8-GFP/+*). Time listed in minutes. Images were acquired every 5.5 mins with a 20x objective. Anterior is to the right. Scale bar = 50 $\mu$ m. The control cluster displays single front-oriented protrusions that extend and retract throughout the migration.

**Movie 2. *fascin*-null border cell migration.** Inverted video of S9 *fascin*-null follicle (*fascin*<sup>sn28/sn28</sup>; *slbo*>*mCD8-GFP/+*). Time listed in minutes. Images were acquired every 5 mins with a 20x objective. Anterior is to the right. Scale bar = 50 $\mu$ m. The *fascin*-null cluster displays aberrant protrusion extensions with many protrusions extending at the same time and from the sides and back of the cluster.

**Movie 3. Control border cell delamination.** Inverted video of early S9 control follicle (*fascin*<sup>sn28/+</sup>; *slbo*>*mCD8-GFP/+*). Time listed in minutes. Images were acquired every 5 mins with a 20x objective. Anterior is to the right. Scale bar = 50 $\mu$ m. The control cluster delaminates considerably faster (104min) than the *fascin*-null follicle (Movie 4).

**Movie 4. *fascin*-null border cell delamination.** Inverted video of early S9 *fascin*-null follicle (*fascin*<sup>sn28/sn28</sup>; *slbo*>*mCD8-GFP/+*). Time listed in minutes. Images were acquired every 5 mins with a 20x objective. Anterior is to the right. Scale bar = 50 $\mu$ m. The *fascin*-null cluster delaminates significantly slower (390min) than the control follicle (Movie 3).

## References:

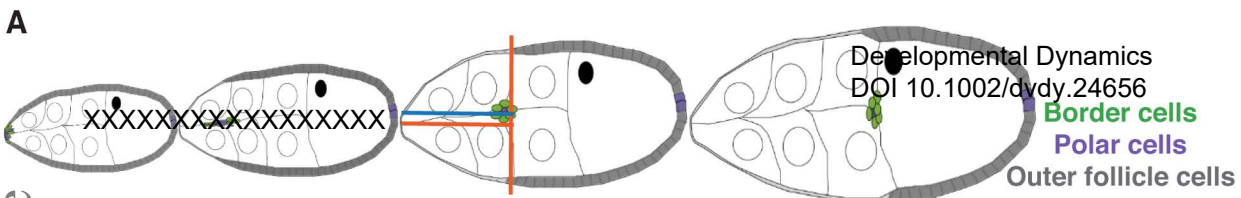
1. Jayo A, Parsons M. Fascin: a key regulator of cytoskeletal dynamics. *Int J Biochem Cell Biol.* 2010;42(10):1614-1617.
2. Hashimoto Y, Kim DJ, Adams JC. The roles of fascins in health and disease. *J Pathol.* 2011;224(3):289-300.
3. Zanet J, Jayo A, Plaza S, Millard T, Parsons M, Stramer B. Fascin promotes filopodia formation independent of its role in actin bundling. *J Cell Biol.* 2012;197(4):477-486.
4. Li A, Dawson JC, Forero-Vargas M, et al. The actin-bundling protein fascin stabilizes actin in invadopodia and potentiates protrusive invasion. *Curr Biol.* 2010;20(4):339-345.
5. Adams JC. Roles of fascin in cell adhesion and motility. *Curr Opin Cell Biol.* 2004;16(5):590-596.
6. Villari G, Jayo A, Zanet J, et al. A direct interaction between fascin and microtubules contributes to adhesion dynamics and cell migration. *Journal of Cell Science.* 2015;128(24):4601-4614.

7. Jayo A, Malboubi M, Antoku S, et al. Fascin Regulates Nuclear Movement and Deformation in Migrating Cells. *Dev Cell.* 2016;38(4):371-383.
8. Anilkumar N, Parsons M, Monk R, Ng T, Adams JC. Interaction of fascin and protein kinase Calpha: a novel intersection in cell adhesion and motility. *EMBO J.* 2003;22(20):5390-5402.
9. Winkelman JD, Bilancia CG, Peifer M, Kovar DR. Ena/VASP Enabled is a highly processive actin polymerase tailored to self-assemble parallel-bundled F-actin networks with Fascin. *Proc Natl Acad Sci U S A.* 2014;111(11):4121-4126.
10. Hashimoto Y, Parsons M, Adams JC. Dual actin-bundling and protein kinase C-binding activities of fascin regulate carcinoma cell migration downstream of Rac and contribute to metastasis. *Mol Biol Cell.* 2007;18(11):4591-4602.
11. Jayo A, Parsons M, Adams JC. A novel Rho-dependent pathway that drives interaction of fascin-1 with p-Lin-11/Isl-1/Mec-3 kinase (LIMK) 1/2 to promote fascin-1/actin binding and filopodia stability. *BMC Biol.* 2012;10:72.
12. Harker AJ, Katkar HH, Bidone TC, et al. Ena/VASP processive elongation is modulated by avidity on actin filaments bundled by the filopodia cross-linker fascin. *Mol Biol Cell.* 2019;30(7):851-862.
13. Hashimoto Y, Skacel M, Adams JC. Roles of fascin in human carcinoma motility and signaling: prospects for a novel biomarker? *Int J Biochem Cell Biol.* 2005;37(9):1787-1804.
14. Cohan CS, Welnhofer EA, Zhao L, Matsumura F, Yamashiro S. Role of the actin bundling protein fascin in growth cone morphogenesis: localization in filopodia and lamellipodia. *Cell Motil Cytoskeleton.* 2001;48(2):109-120.
15. Ma Y, Li A, Faller WJ, et al. Fascin 1 is transiently expressed in mouse melanoblasts during development and promotes migration and proliferation. *Development.* 2013;140(10):2203-2211.
16. De Arcangelis A, Georges-Labouesse E, Adams JC. Expression of fascin-1, the gene encoding the actin-bundling protein fascin-1, during mouse embryogenesis. *Gene Expr Patterns.* 2004;4(6):637-643.
17. Arlt MJ, Kuzmanov A, Snedeker JG, Fuchs B, Silvan U, Sabile AA. Fascin-1 enhances experimental osteosarcoma tumor formation and metastasis and is related to poor patient outcome. *BMC Cancer.* 2019;19(1):83.
18. Spradling A. Developmental genetics of oogenesis. In. The development of Drosophila melanogaster: Cold Spring Harbor Laboratory Press; 1993:1-70.
19. Montell DJ. Border-cell migration: The race is on. *Nat Rev Mol Cell Bio.* 2003;4(1):13-24.
20. Montell DJ, Yoon WH, Starz-Gaiano M. Group choreography: mechanisms orchestrating the collective movement of border cells. *Nat Rev Mol Cell Biol.* 2012;13(10):631-645.
21. Cai D, Chen SC, Prasad M, et al. Mechanical feedback through E-cadherin promotes direction sensing during collective cell migration. *Cell.* 2014;157(5):1146-1159.

22. Prasad M, Montell DJ. Cellular and molecular mechanisms of border cell migration analyzed using time-lapse live-cell imaging. *Dev Cell.* 2007;12(6):997-1005.
23. Fulga TA, Rorth P. Invasive cell migration is initiated by guided growth of long cellular extensions. *Nat Cell Biol.* 2002;4(9):715-719.
24. Montell DJ, Rorth P, Spradling AC. slow border cells, a locus required for a developmentally regulated cell migration during oogenesis, encodes Drosophila C/EBP. *Cell.* 1992;71(1):51-62.
25. Cant K, Knowles BA, Mooseker MS, Cooley L. Drosophila Singed, a Fascin Homolog, Is Required for Actin Bundle Formation during Oogenesis and Bristle Extension. *Journal of Cell Biology.* 1994;125(2):369-380.
26. Cant K, Cooley L. Single amino acid mutations in Drosophila fascin disrupt actin bundling function in vivo. *Genetics.* 1996;143(1):249-258.
27. Aranjuez G, Burtscher A, Sawant K, Majumder P, McDonald JA. Dynamic myosin activation promotes collective morphology and migration by locally balancing oppositional forces from surrounding tissue. *Mol Biol Cell.* 2016;27(12):1898-1910.
28. Cai D, Dai W, Prasad M, Luo J, Gov NS, Montell DJ. Modeling and analysis of collective cell migration in an in vivo three-dimensional environment. *Proc Natl Acad Sci U S A.* 2016;113(15):E2134-2141.
29. Rorth P. Gal4 in the Drosophila female germline. *Mech Dev.* 1998;78(1-2):113-118.
30. Barth JM, Hafen E, Kohler K. The lack of autophagy triggers precocious activation of Notch signaling during Drosophila oogenesis. *BMC Dev Biol.* 2012;12:35.
31. Aranjuez G, Kudlaty E, Longworth MS, McDonald JA. On the role of PDZ domain-encoding genes in Drosophila border cell migration. *G3 (Bethesda).* 2012;2(11):1379-1391.
32. Bender HA. Studies on the Expression of Various Singed Alleles in Drosophila Melanogaster. *Genetics.* 1960;45(7):867-883.
33. Gates J, Nowotarski SH, Yin H, et al. Enabled and Capping protein play important roles in shaping cell behavior during Drosophila oogenesis. *Dev Biol.* 2009;333(1):90-107.
34. Bianco A, Poukkula M, Cliffe A, et al. Two distinct modes of guidance signalling during collective migration of border cells. *Nature.* 2007;448(7151):362-365.
35. Sawant K, Chen Y, Kotian N, Preuss KM, McDonald JA. Rap1 GTPase promotes coordinated collective cell migration in vivo. *Mol Biol Cell.* 2018;29(22):2656-2673.
36. De Graeve FM, Van de Bor V, Ghiglione C, et al. Drosophila apc regulates delamination of invasive epithelial clusters. *Dev Biol.* 2012;368(1):76-85.
37. Niewiadomska P, Godt D, Tepass U. DE-Cadherin is required for intercellular motility during Drosophila oogenesis. *J Cell Biol.* 1999;144(3):533-547.
38. Hayashi Y, Osanai M, Lee GH. Fascin-1 expression correlates with repression of E-cadherin expression in hepatocellular carcinoma cells and augments their invasiveness in combination with matrix metalloproteinases. *Cancer Sci.* 2011;102(6):1228-1235.

39. Fox EF, Lamb MC, Mellentine SQ, Tootle TL. Prostaglandins regulate invasive, collective border cell migration. *bioRxiv*. 2019;821686.
40. Rittie L. Cellular mechanisms of skin repair in humans and other mammals. *J Cell Commun Signal*. 2016;10(2):103-120.
41. Stuelten CH, Parent CA, Montell DJ. Cell motility in cancer invasion and metastasis: insights from simple model organisms. *Nat Rev Cancer*. 2018;18(5):296-312.
42. Elkhatib N, Neu MB, Zensen C, et al. Fascin plays a role in stress fiber organization and focal adhesion disassembly. *Curr Biol*. 2014;24(13):1492-1499.
43. Groen CM, Spracklen AJ, Fagan TN, Tootle TL. Drosophila Fascin is a novel downstream target of prostaglandin signaling during actin remodeling. *Mol Biol Cell*. 2012;23(23):4567-4578.
44. Alam H, Bhate AV, Gangadaran P, et al. Fascin overexpression promotes neoplastic progression in oral squamous cell carcinoma. *BMC Cancer*. 2012;12:32.
45. Bear JE, Loureiro JJ, Libova I, Fassler R, Wehland J, Gertler FB. Negative regulation of fibroblast motility by Ena/VASP proteins. *Cell*. 2000;101(7):717-728.
46. Adams JC, Clelland JD, Collett GD, Matsumura F, Yamashiro S, Zhang L. Cell-matrix adhesions differentially regulate fascin phosphorylation. *Mol Biol Cell*. 1999;10(12):4177-4190.
47. Wang H, Qiu Z, Xu Z, et al. aPKC is a key polarity determinant in coordinating the function of three distinct cell polarities during collective migration. *Development*. 2018;145(9).
48. Peppelenbosch MP, Tertoolen LG, Hage WJ, de Laat SW. Epidermal growth factor-induced actin remodeling is regulated by 5-lipoxygenase and cyclooxygenase products. *Cell*. 1993;74(3):565-575.
49. Bulin C, Albrecht U, Bode JG, et al. Differential effects of vasodilatory prostaglandins on focal adhesions, cytoskeletal architecture, and migration in human aortic smooth muscle cells. *Arterioscler Thromb Vasc Biol*. 2005;25(1):84-89.
50. Tamma G, Wiesner B, Furkert J, et al. The prostaglandin E2 analogue sulprostone antagonizes vasopressin-induced antidiuresis through activation of Rho. *J Cell Sci*. 2003;116(Pt 16):3285-3294.
51. Tootle TL. Genetic insights into the in vivo functions of prostaglandin signaling. *Int J Biochem Cell Biol*. 2013;45(8):1629-1632.
52. Groen CM. *Novel regulation and function of the actin bundling protein Fascin*, University of Iowa; 2015.
53. Spracklen AJ, Kelpsch DJ, Chen X, Spracklen CN, Tootle TL. Prostaglandins temporally regulate cytoplasmic actin bundle formation during Drosophila oogenesis. *Mol Biol Cell*. 2014;25(3):397-411.
54. Friedl P, Gilmour D. Collective cell migration in morphogenesis, regeneration and cancer. *Nat Rev Mol Cell Biol*. 2009;10(7):445-457.

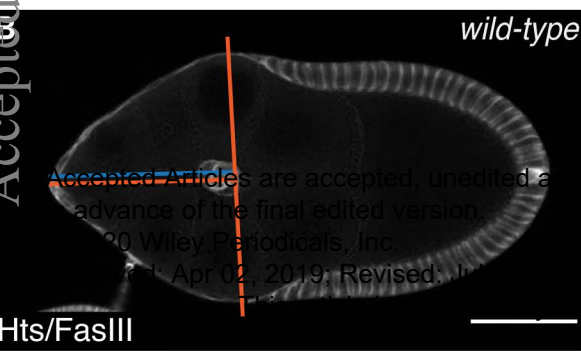
55. Gross SR. Actin binding proteins: their ups and downs in metastatic life. *Cell Adh Migr.* 2013;7(2):199-213.
56. Yoder BJ, Tso E, Skacel M, et al. The expression of fascin, an actin-bundling motility protein, correlates with hormone receptor-negative breast cancer and a more aggressive clinical course. *Clin Cancer Res.* 2005;11(1):186-192.
57. Telley IA, Gaspar I, Ephrussi A, Surrey T. Aster migration determines the length scale of nuclear separation in the Drosophila syncytial embryo. *J Cell Biol.* 2012;197(7):887-895.
58. Zanet J, Stramer B, Millard T, Martin P, Payre F, Plaza S. Fascin is required for blood cell migration during Drosophila embryogenesis. *Development.* 2009;136(15):2557-2565.
59. Zaccai M, Lipshitz HD. Differential distributions of two adducin-like protein isoforms in the Drosophila ovary and early embryo. *Zygote.* 1996;4(2):159-166.
60. Patel NH, Snow PM, Goodman CS. Characterization and cloning of fasciclin III: a glycoprotein expressed on a subset of neurons and axon pathways in Drosophila. *Cell.* 1987;48(6):975-988.
61. Oda H, Uemura T, Harada Y, Iwai Y, Takeichi M. A Drosophila homolog of cadherin associated with armadillo and essential for embryonic cell-cell adhesion. *Dev Biol.* 1994;165(2):716-726.
62. Platt JL, Michael AF. Retardation of fading and enhancement of intensity of immunofluorescence by p-phenylenediamine. *J Histochem Cytochem.* 1983;31(6):840-842.
63. Abramoff MD, Magalhaes P, Ram S. Image processing with ImageJ. *Biophotonics Int.* 2004;11:36-42.



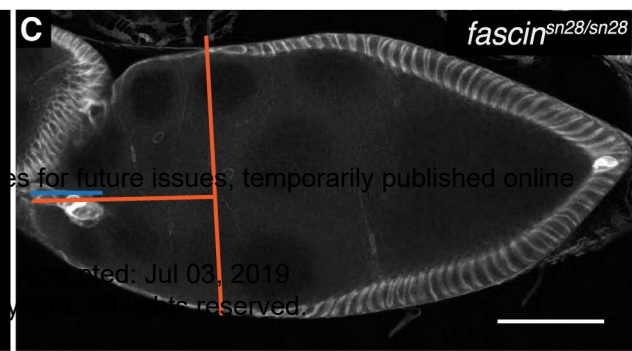
— distance of border cells      — distance of outer follicle cells

**Migration Index= Distance of border cells ( $\mu\text{m}$ )  $\div$  Distance of outer follicle cells ( $\mu\text{m}$ )**

On-time migration:  $\sim 1$     Delayed migration:  $<1$     Accelerated migration:  $>1$



Migration Index= **92.59 / 94.64 = 0.97**



Migration Index= **36.93 / 102.02 = 0.36**

Developmental Dynamics  
DOI 10.1002/dvdy.24656

**Border cells**

**Polar cells**

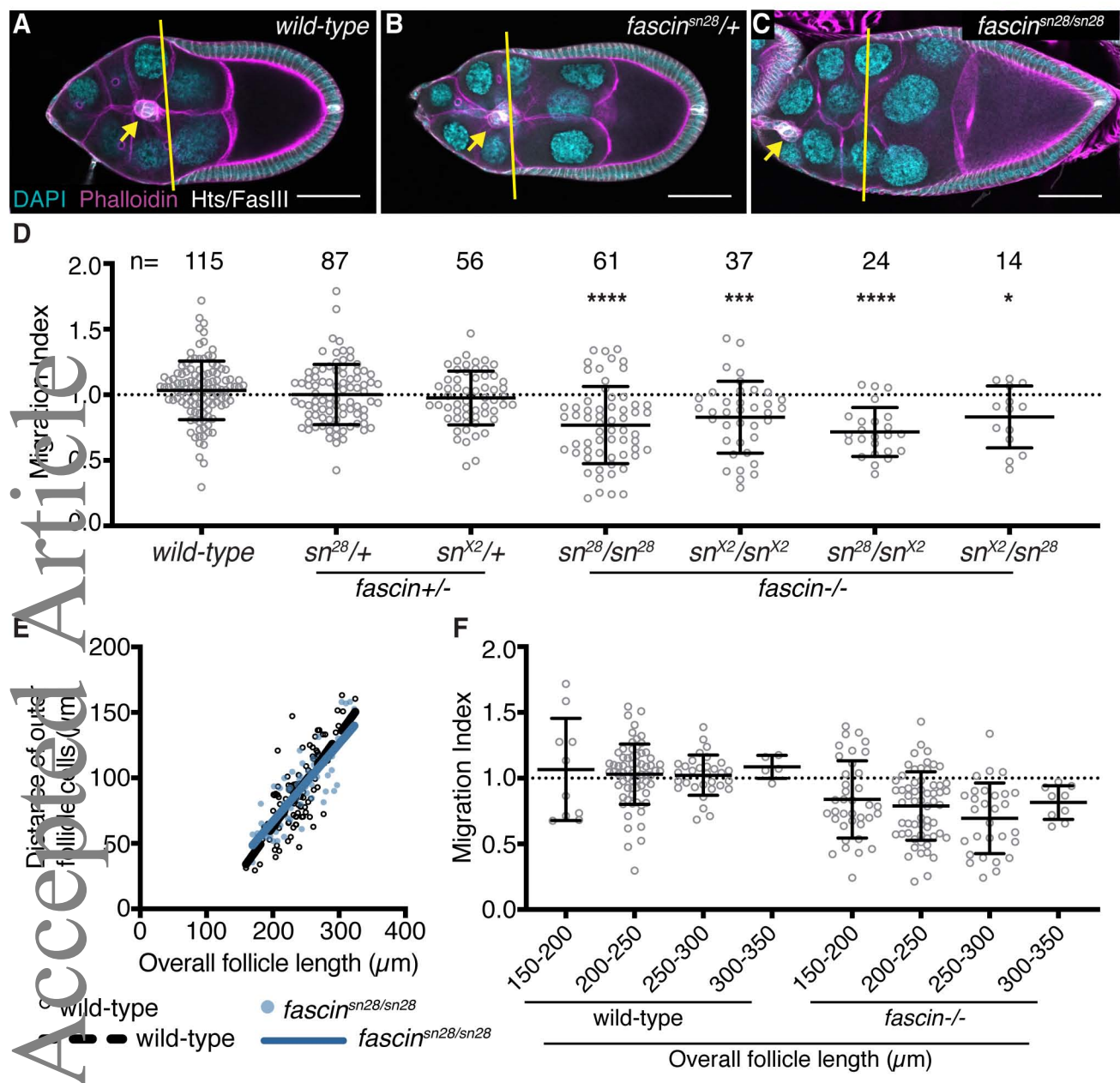
**Outer follicle cells**

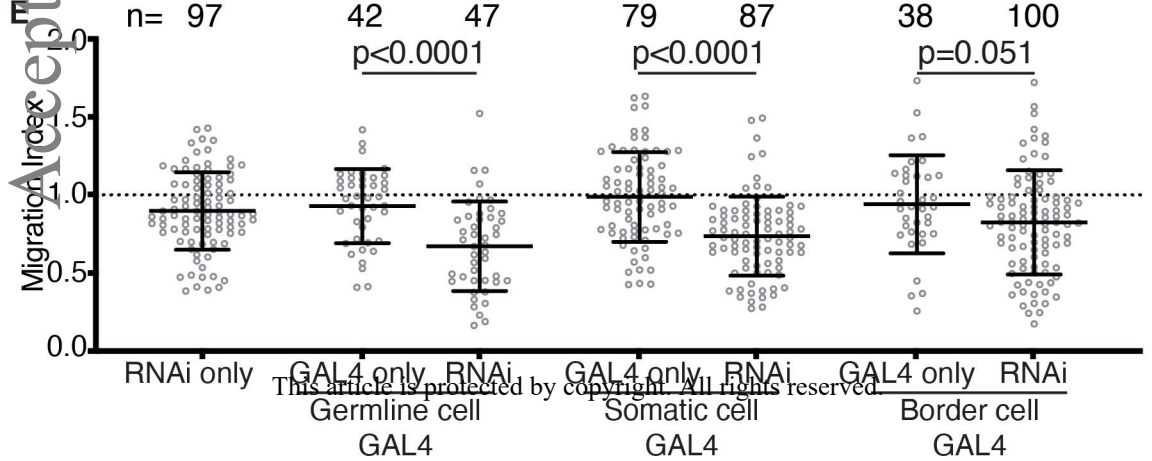
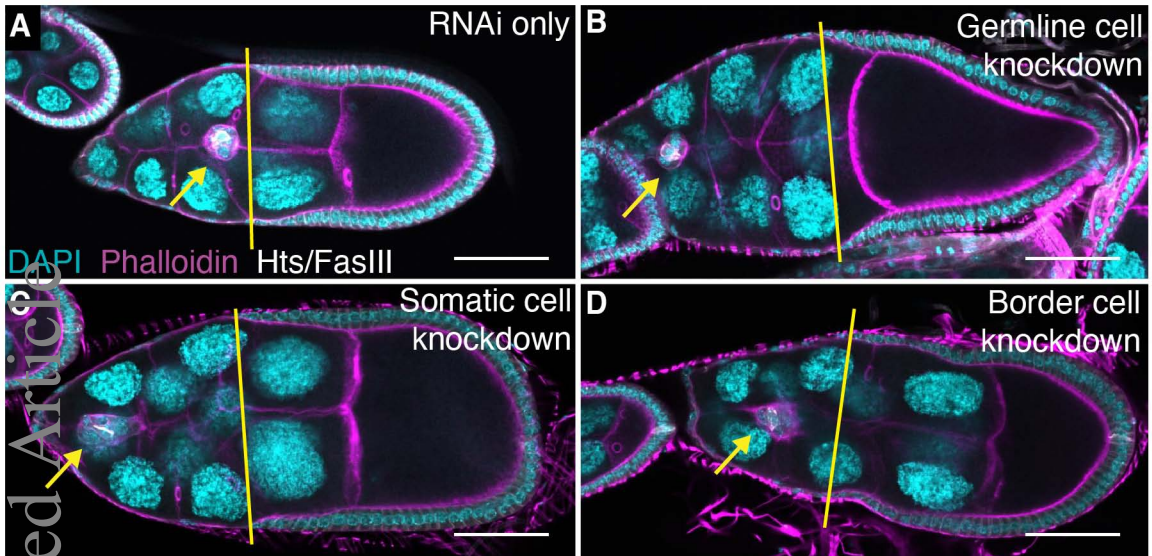
Accepted Articles are accepted, unedited articles for future issues, temporarily published online in advance of the final edited version.

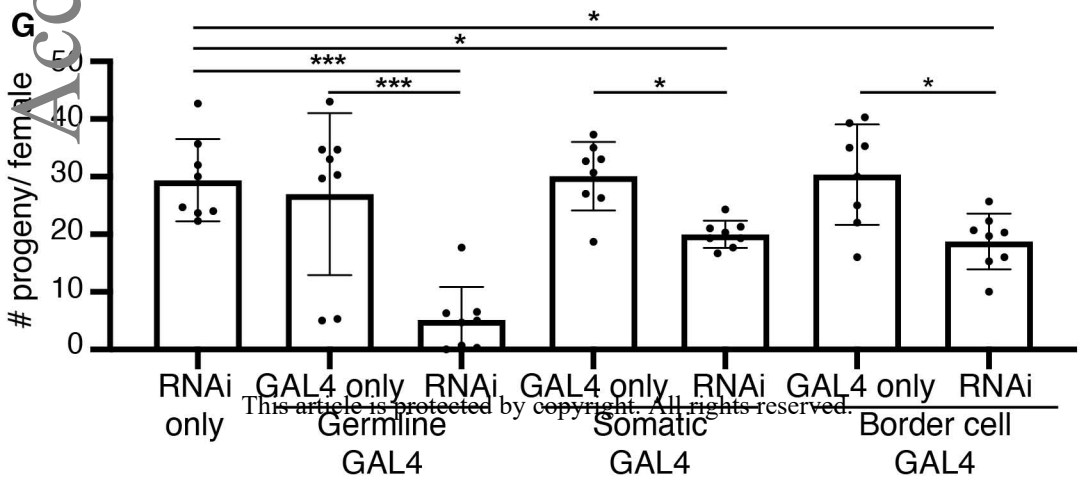
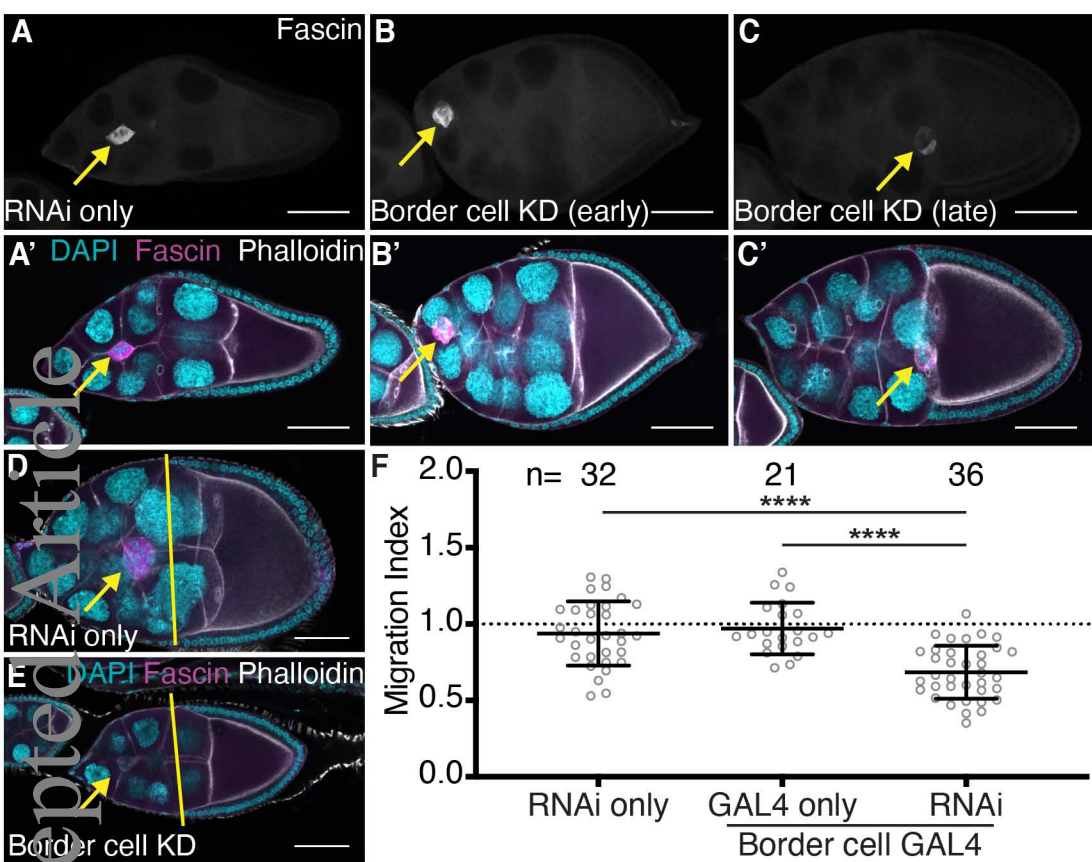
© 2019 Wiley Periodicals, Inc.

Received: Apr 02, 2019; Revised: Jun 25, 2019; Accepted: Jul 03, 2019

All rights reserved.



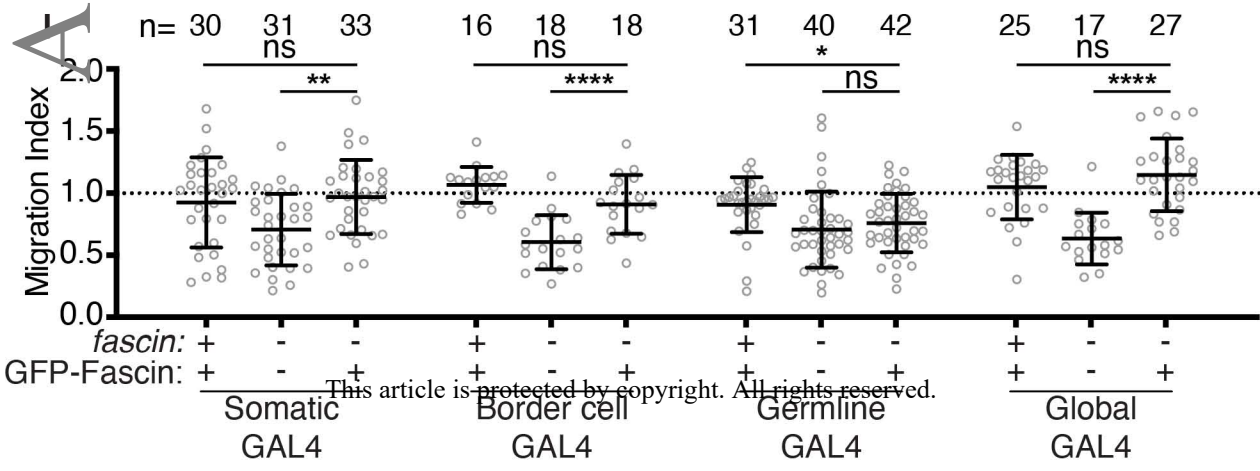
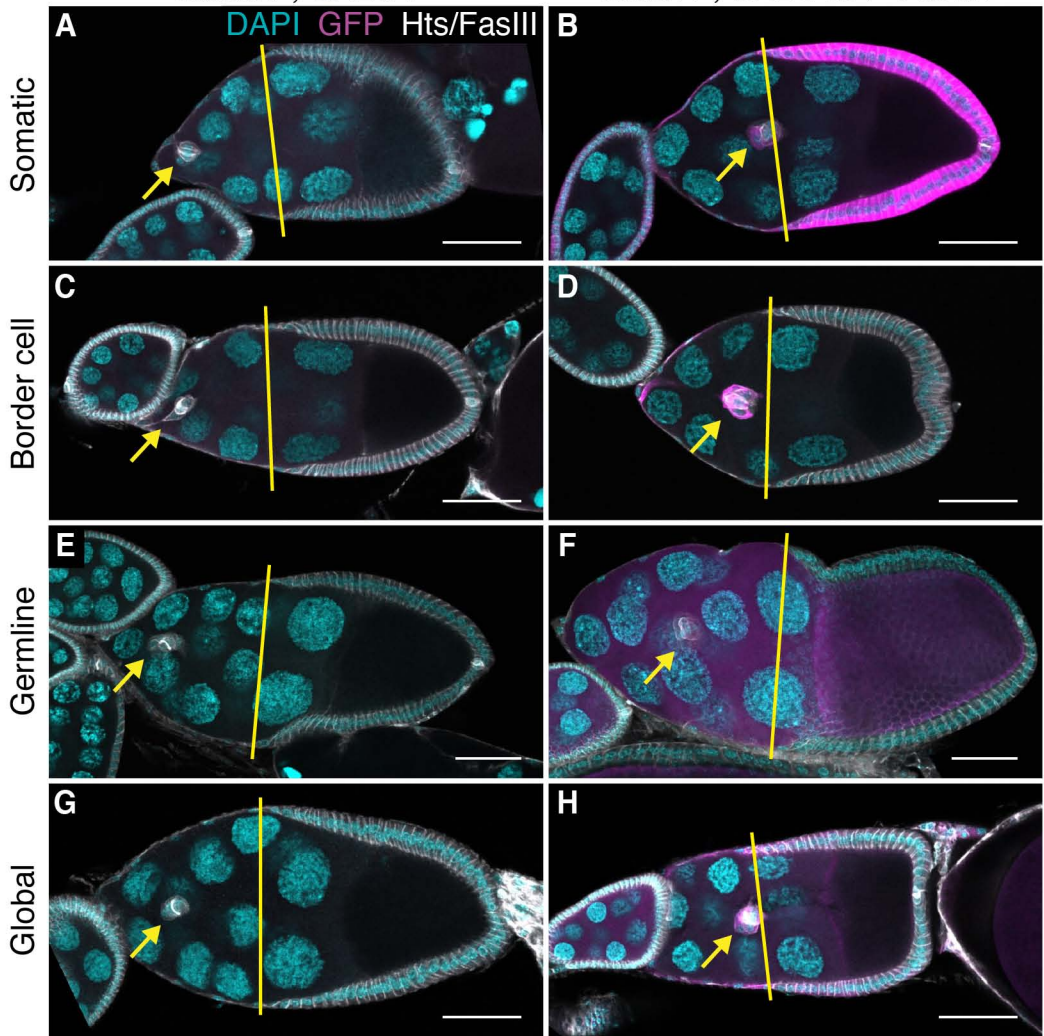




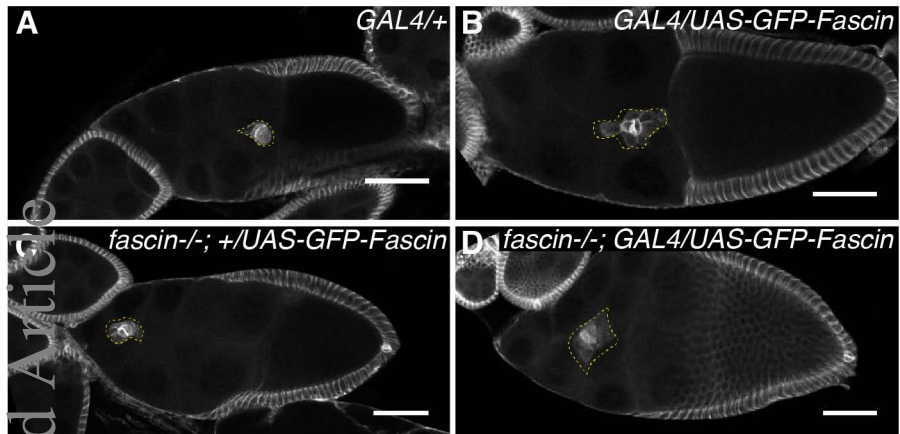
# Accepted Article

*fascin*-/-; GAL4/+

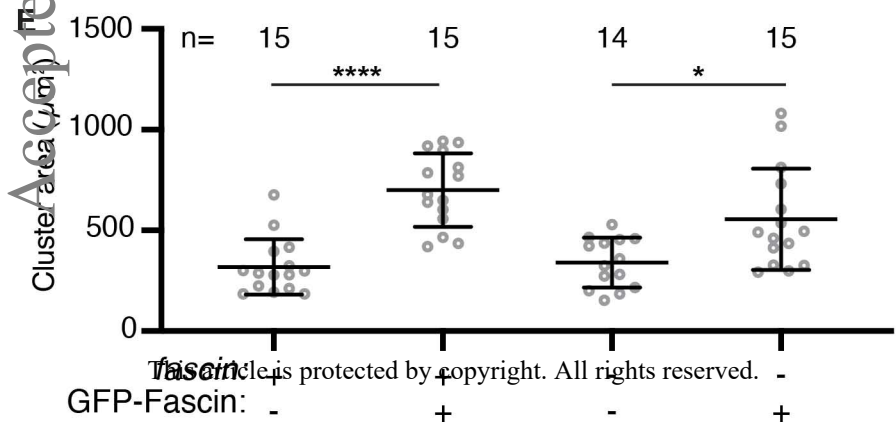
*fascin*-/-; GAL4/GFP-Fascin

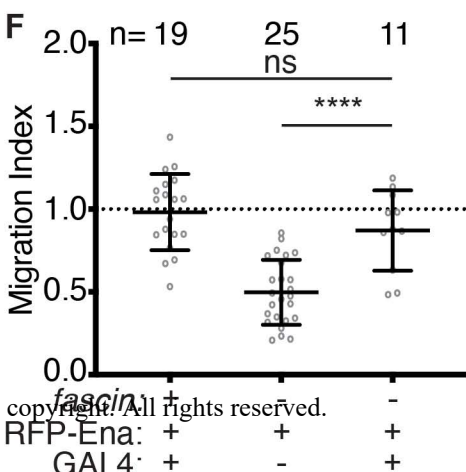
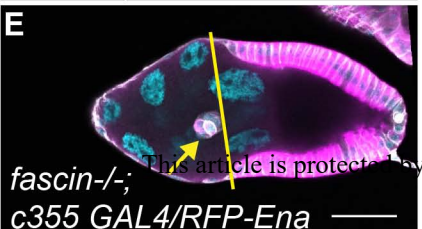
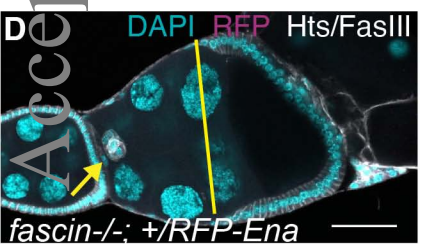
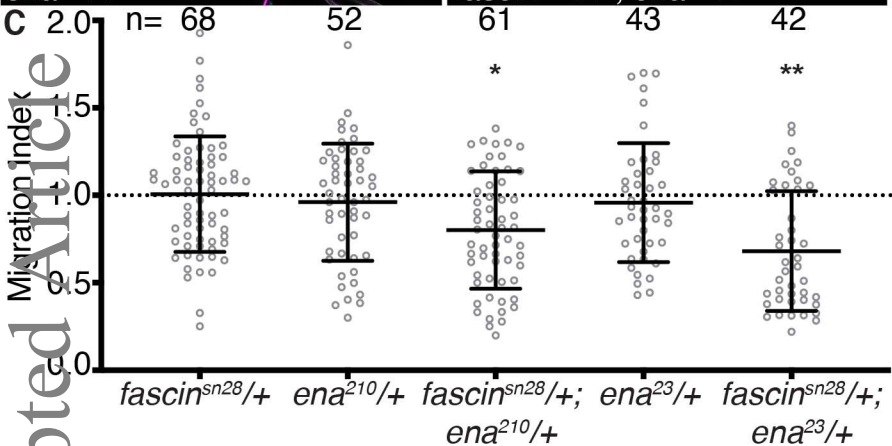
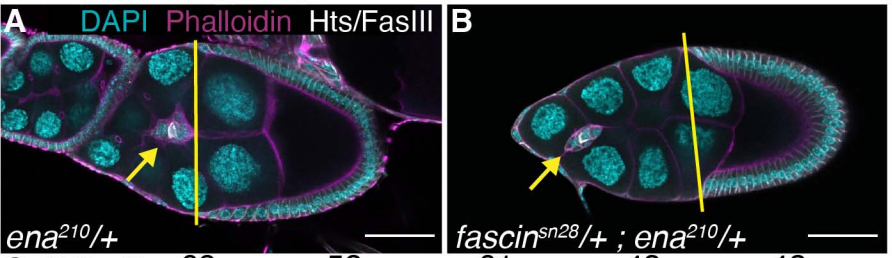


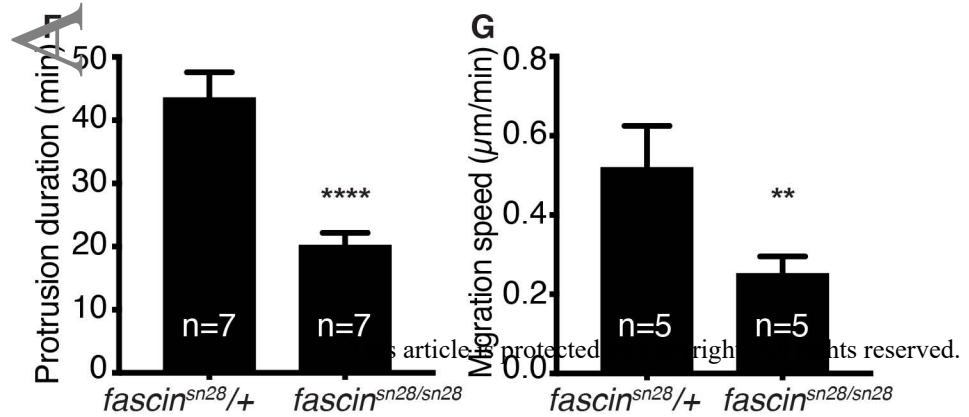
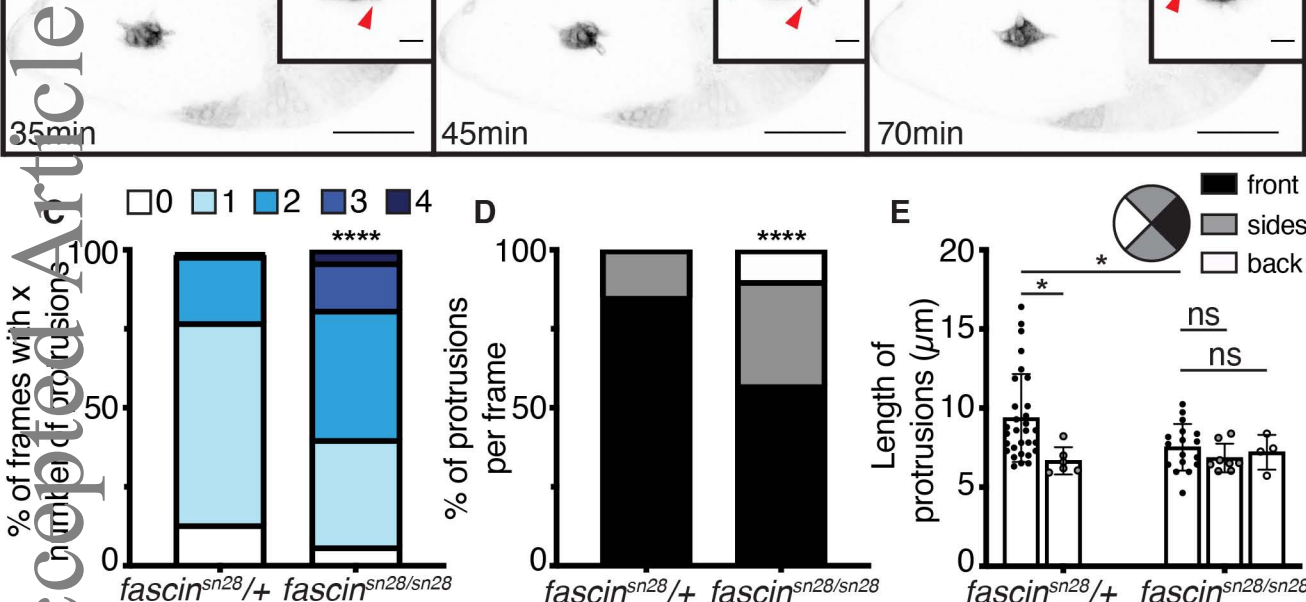
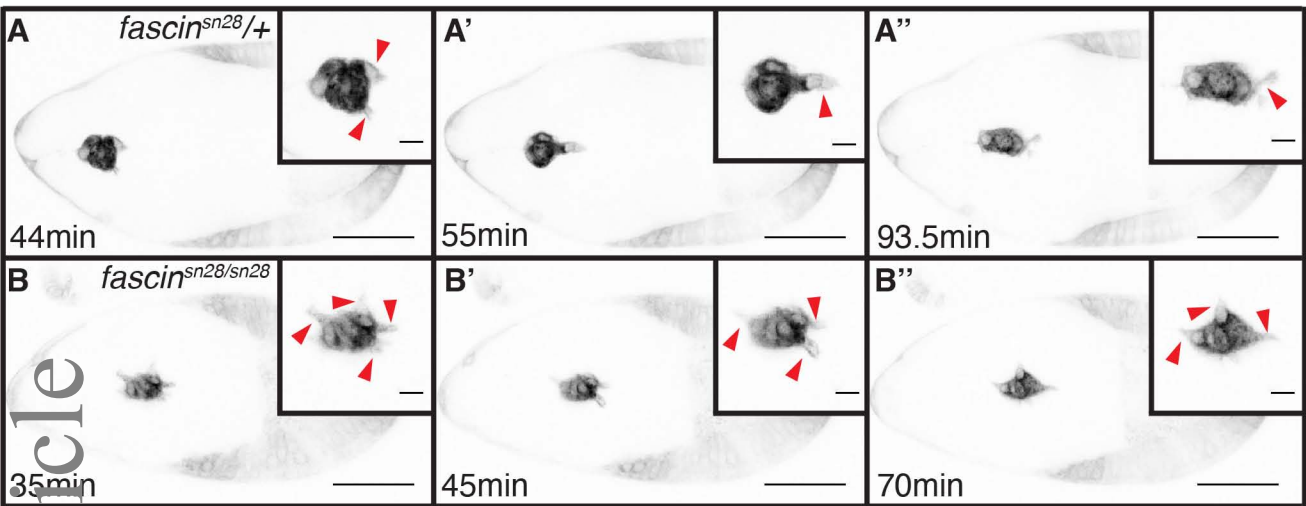
# Germline GAL4

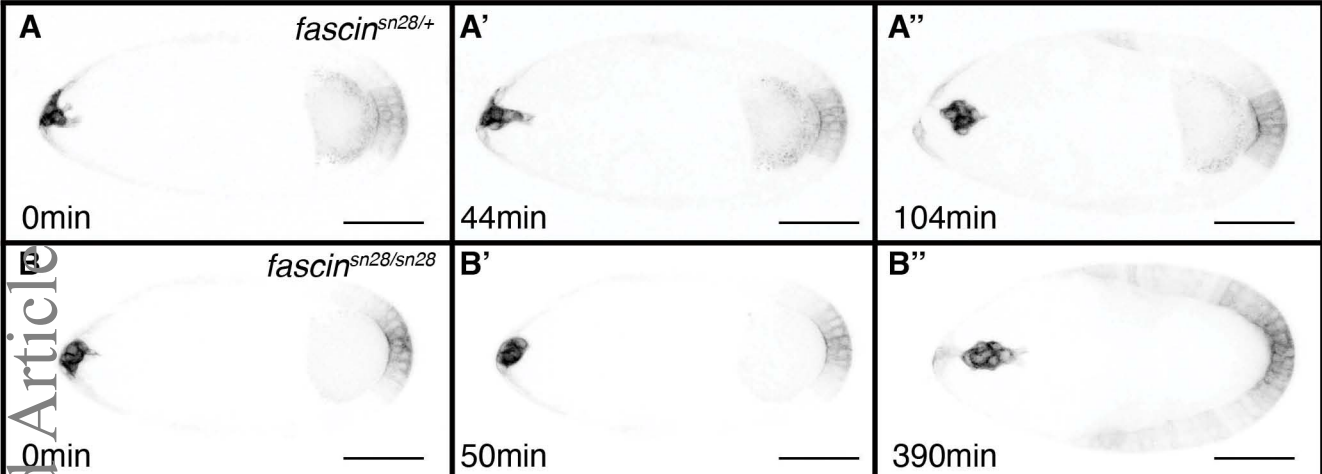


Accepted Article



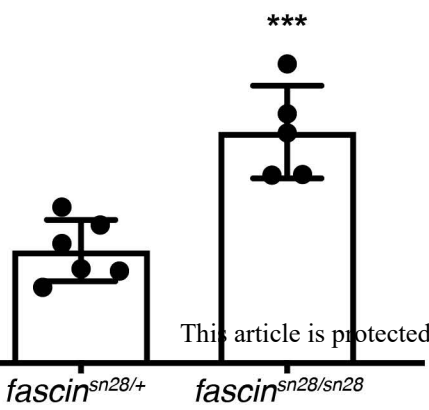






Accepted Article

### Live Imaging



### D

